Chapter 7

Calibration of Numerical Model

Calibration of the numerical model was performed through a series of experiments that will be explained shortly in sections 4.1 and 4.2. Single stack experiments are aimed understanding the effect of some basic variables, described in each pertinent section, whilst three stacks configuration has the main goal of identifying contact.

7.1 Seven-tiers Single Stack (7x1)

The study limited the analysis of displacement of top corner of some individual containers. Furthermore, for means of comparison the highest container was used for evaluation purposes. As mentioned in section 2.5, displacement-time response data was analyzed using three techniques: time history, coefficients of Fourier expansion and RMS value comparison.

7.1.1 Numerical Investigation: Finite Element Analysis (7x1)

A simplified 3-D finite element model of the system is as follows: seven scaled models of a 20 ft ISO freight dry container, twist locks and shaking table arranged in a single stack of seven-tiers. This model was developed using commercial software (Hypermesh 8.0, Altair Engineering Inc., 1995-2006). Details of the model's structure are presented in section 5.1. Scaled models were considered as steel frames sections compounded of circular and pipe beams (details of every profile are described in table 5.1). Numerical model is depicted in Figure 7.1. Moreover, twist locks were modeled using the mathematical relationship depicted in Figure 5.7.

Finally, the shaking table was considered a rigid body where the driving excitation follows same conditions imposed in the experiments (see table 4.1). Damping for the

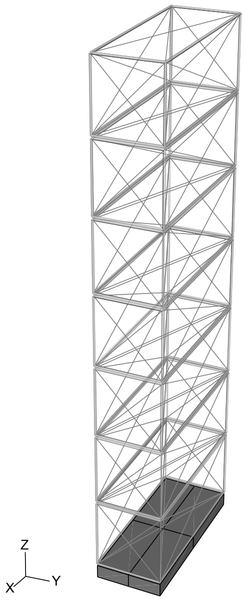

Figure 7.1: Finite element model of the seven-tier single stack case (7x1).

system was implemented using Rayleigh damping coefficients (see section 5.3.1) characterizing the main difference between this model and the model used during the pilot study. The numerical analysis was performed with a commercial finite element analysis package (Abaqus version 6.7, Dassault Systems), which accounts for geometry non-linearity considering a dynamic study in an implicit integration scheme.

7.1.2 Numerical Model Validation (7x1)

7.1.2.1 Amplitude (7x1)

Naturally, amplitude affects the system in a manner proportional to its magnitude, i.e., an increase in the amplitude of the driving excitation induces a direct proportional increase in the response amplitude observed in point 1. However, this does not provide any extra information about the nature of the system. To visualize the system, the overall behavior a plot of a non-dimensional ratio between driving excitation and response versus driving excitation was used. Response amplitude was calculated using Fourier expansion as explained earlier in section 2.5. Figure 7.2 depicts this kind of comparison. The corresponding values for the experimental data were 0.253, 0.162, and 0.155 , for the driving excitation amplitudes of 2, 4 and 6 mm, respectively. These measurements are consistent with the finite element prediction that were 0.219, 0.156 and 0.157 for the same amplitude range. Differences between experimental and numerical data were 13.59%, 3.6%

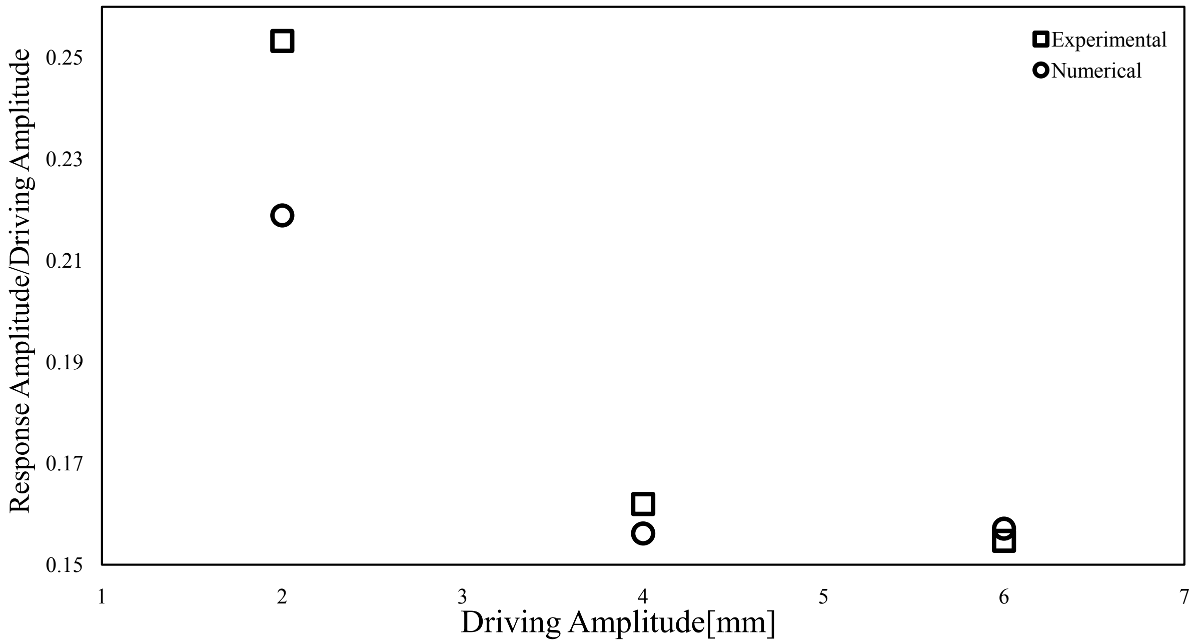

Figure 7.2: Amplitude comparison (relative motion). Case: 7x1–2 Hz–1 mm gap–0 degree.

and 1.54% for the driving excitation amplitudes of 2, 4 and 6 mm, respectively. For this variable the numerical data shows a good level of agreement with the experimental data. Furthermore, Figure 7.2 points out a stable system, a fact that is reflected between experimental and numerical data. Additionally, the same behavior was observed for the range of frequencies used in this study. Although the frequency range is not relevant for ships' movements like rolling and pitching that have frequencies ranging from 0.1 to 0.04 Hz, the same cannot be assumed for heaving. Thus, findings originated from the frequency range of this study can be used to understand the mechanical behavior of the container stack during heaving. Another interesting study involving the ratio described here is the plot against the ratio between driving excitation frequency and natural frequency of the system, which characterizes the *transmissibility* function. However, for such an approach, the estimation of the natural frequencies of the system would be necessary. Nevertheless, the system itself is non-linear, so a classical eigenvalue approach to find the natural frequencies does not apply, which leaves experimental determination as the only option.

7.1.2.2 Frequency (7x1)

Frequency analysis shows that the corresponding values for the experimental data were 0.25, 0.15, and 2.44 mm, for the lateral direction and 0.85,0.82 and 0.42 mm for the vertical direction for the frequencies of 0.5, 1 and 5 Hz, respectively. These measurements are consistent with the finite element prediction that were 0.29, 0.20 and 2.13 mm for the lateral direction and 0.89, 0.77 and 0.51 mm for the vertical direction for the same frequency range. Differences between experimental and numerical data were 16.03%, 32.83% and 12.82% for the lateral direction. For the vertical direction these differences were 5.03%, 6.14% and 20.03%. Differences between numerical and experimental data have origin in the fact that only the first eigenmode of the numerical model (individual container) was a close to the real value measured in a previous experiment. For further details read [44]. Thus authors remained extremely cautious about using the numerical model in a wide frequency range. About the mechanical behavior: the system presents different behavior for every direction. For lateral direction, the system presents a positive effect depending on the frequency, i.e., an increase in frequency induces an increase in the response. On the other hand, the vertical direction presents an opposite behavior: an increase in frequency causes a decrease in the response observed in point 1. Both effects are depicted in Figure 7.3.

7.1.2.3 Payload (7x1)

Experimental and numerical values (RMS) for the relative motion of point 1 for the loaded cases presented in Figure 7.4 were 0.41 and 0.48, respectively, showing a difference of 18.21%. This difference ranges from 15% to 20% for all cases performed. Authors believe that differences in construction for the numerical model are responsible for such differences in RMS. Experiments involving loads employed sand bags fixed to each container floor using cargo belts, while their simulation counterparts, weight was added to the geometrical center. Consequently, both configurations will induce a complete different distribution of moments over the system, increasing differences between experimental and numerical results. Regarding the mechanical behavior: the inclusion of a payload in the stack affects the system negatively, i.e., increase in the payload induced a decrease in the relative motion in point 1, as can be observed in Figures 7.4a and 7.4b. It is important to emphasize that this effect was observed in all experimental and numerical cases for the frequency range studied. However, no study was conducted to analyze the system behavior in frequencies higher than the ones used for the study cases, which could give additional information about the system's behavior. More about payload effect will be explored shortly in section 8.1.

7.1.2.4 Base rotation (7x1)

Analyzing rotation of the base shows that the corresponding values for the experimental data were 0.16, 0.35, 3.76 mm, for the lateral direction and 0.78, 0.35, 0.10 mm for the vertical direction for angles of 0, 2 and 5 degrees, respectively. These measurements

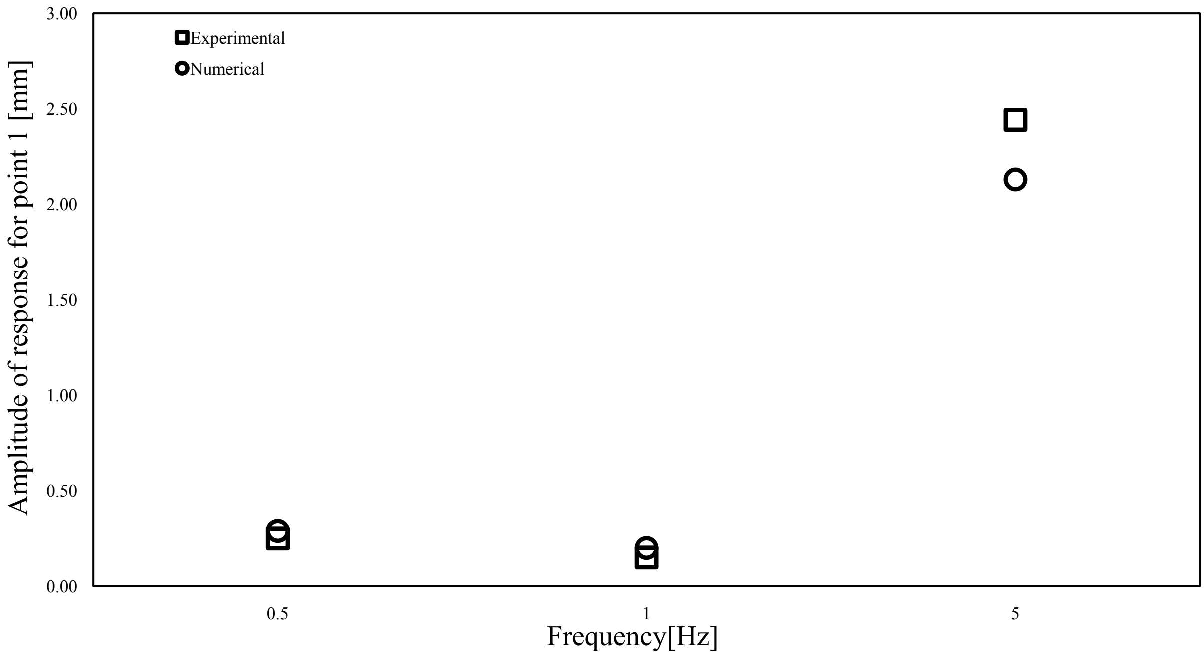

(a) Lateral response.

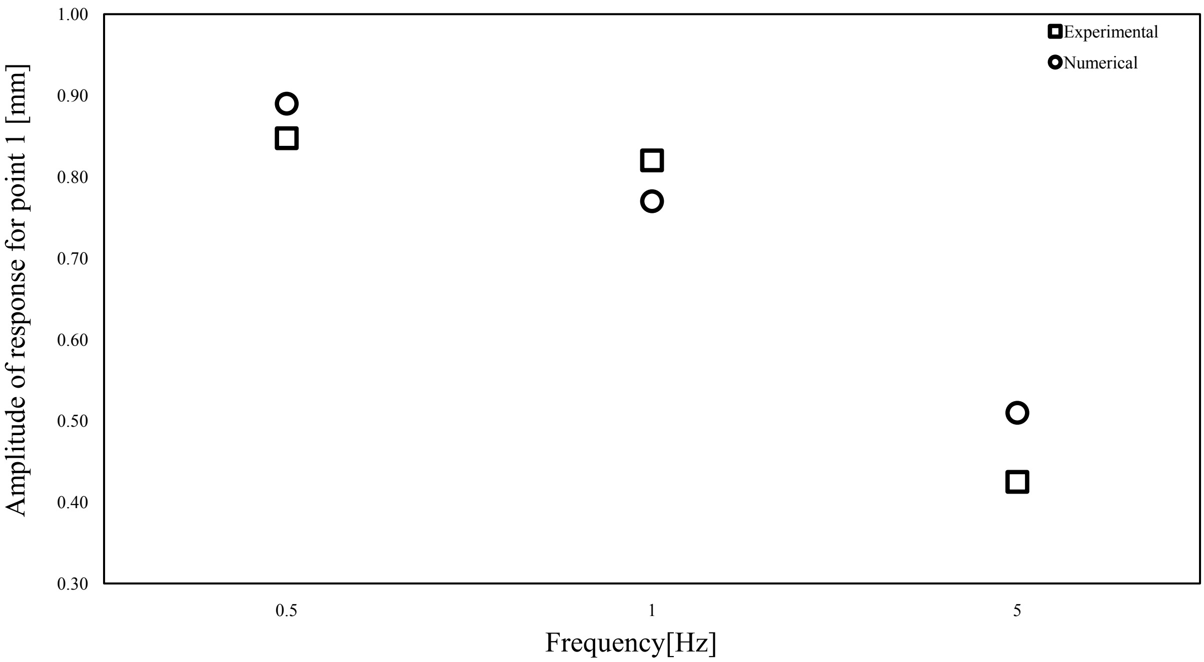

(b) Vertical response.

Figure 7.3: Frequency comparison (relative motion). Case: 7x1–6 mm–1 mm gap–5 degrees.

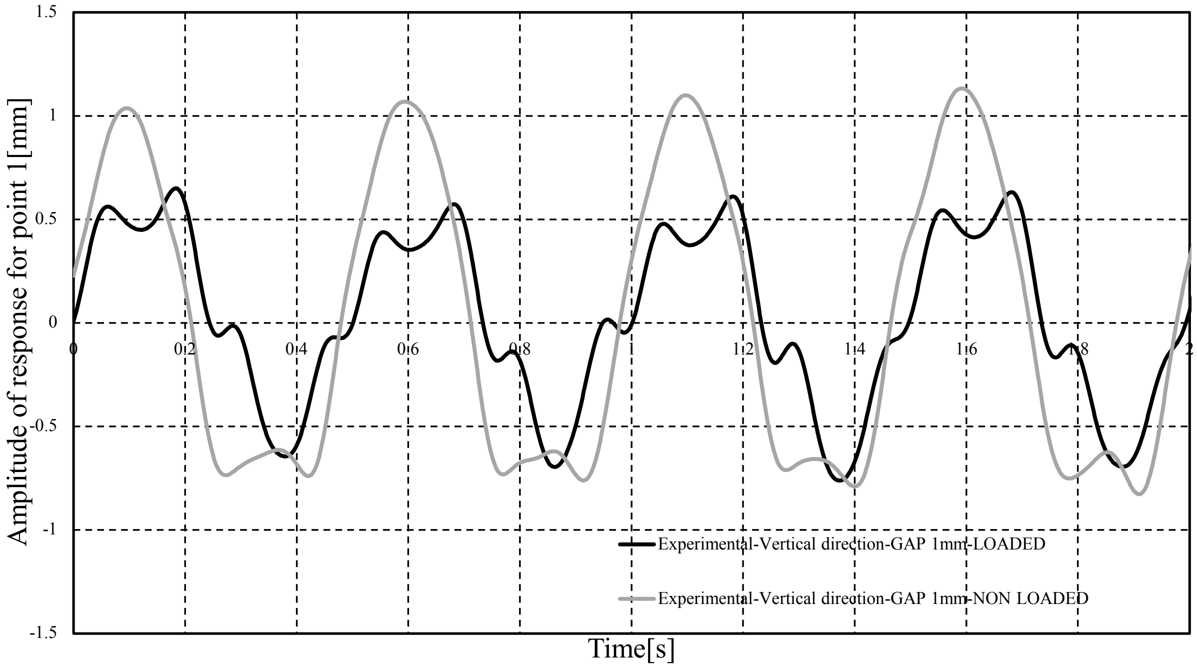

(a) Experimental data.

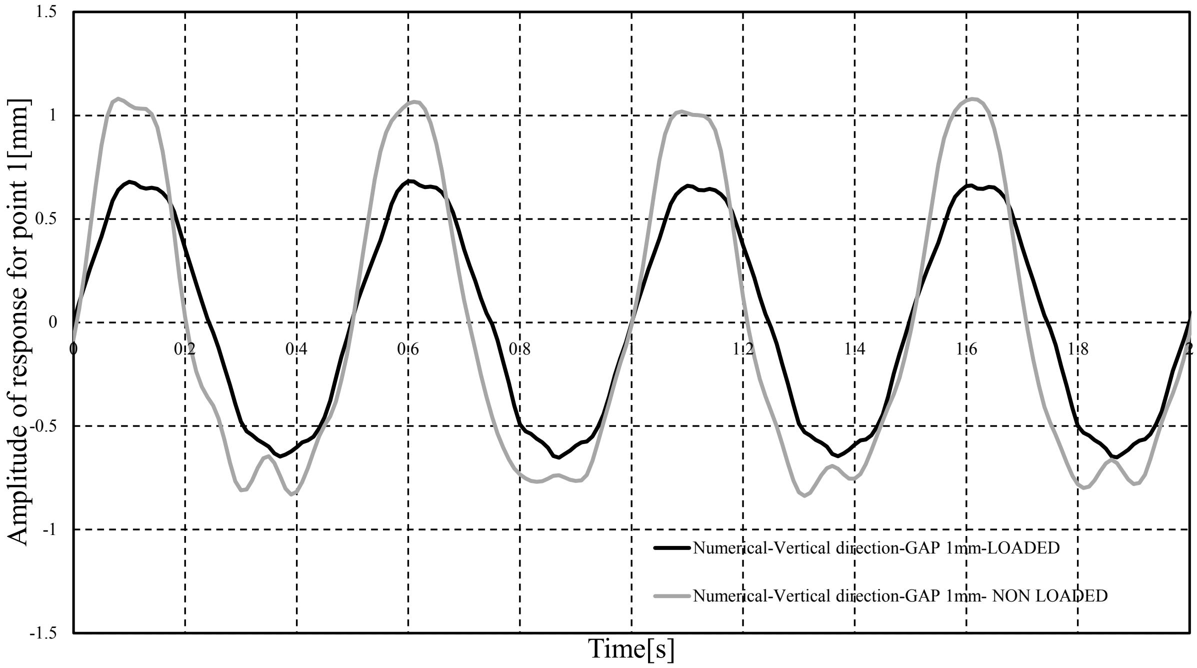

(b) and numerical data.

Figure 7.4: Payload comparison (relative motion). Case: 7x1–6 mm–1 mm gap–0 degree.

are consistent with the finite element prediction that were 0.19, 0.41, 3.95 mm for the lateral direction and 0.75, 0.4, 0.11 mm for the vertical direction for the same frequency range. Differences between experimental and numerical data were 18.35%, 15.58% and 4.96% for the lateral direction and 4.23%, 14.19% and 14.54% for the vertical direction. About the mechanical behavior, rotation of the shaking table in the horizontal direction results in a significant increase in the lateral amplitude observed in point 1 (Figure 7.5a), which corroborates our understanding about the effect of this variable in the response. Contrarily, the vertical direction response decreases with rotation (Figure 7.5b). Inclining the container stack base favors the appearance of an extra lateral component of force (gravity force) besides the driving force, which helps the system to exceed the friction forces acting on the corner castings and consequently increase response.

7.1.2.5 Gap size (7x1)

Changes in the gap size induced the corresponding values (relative motion of point 1) for the experimental data: 0.69 and 1.18 mm, for gap sizes of 1 and 2 mm, respectively. These measurements are consistent with the finite element prediction that were 0.69 and 1.05 mm for the same gap size range. Differences between experimental and numerical data were 0.03% and 10.67%. About the mechanical behavior it can be said that for the range studied, an increase in gap size produces an increase in the response amplitude observed in point 1, as can be observed in Figure 7.6 and 7.7. This is the most interesting finding to emerge from this study. The implications of this finding will be explored in the context applications and advice for the maritime transportation industry in section 8.1.

7.1.3 Discrepancies (7x1)

It is interesting to point out that results for small amplitudes in the experimental and numerical analysis presented some discrepancies for most cases in this study. Such discrepancies can be observed in Figure 7.2 for the amplitude of 2 mm. However, these differences were expected because of many uncertainties and assumptions for the numerical model. Additionally, the experimental data presented some experimental anomalies. Regarding factors in the numerical model that contribute to differences between results, it is important to emphasize the uncertainty regarding the twist locks' vertical and shear stiffness, small differences between the dynamical modes of the scaled and the numerical model, and finally differences between vertical stiffness and geometric features of the numerical model and the scaled container. Additionally, numerical model did not consider contact and consequent friction between corner castings, which is a key point for the lateral response of the stack.

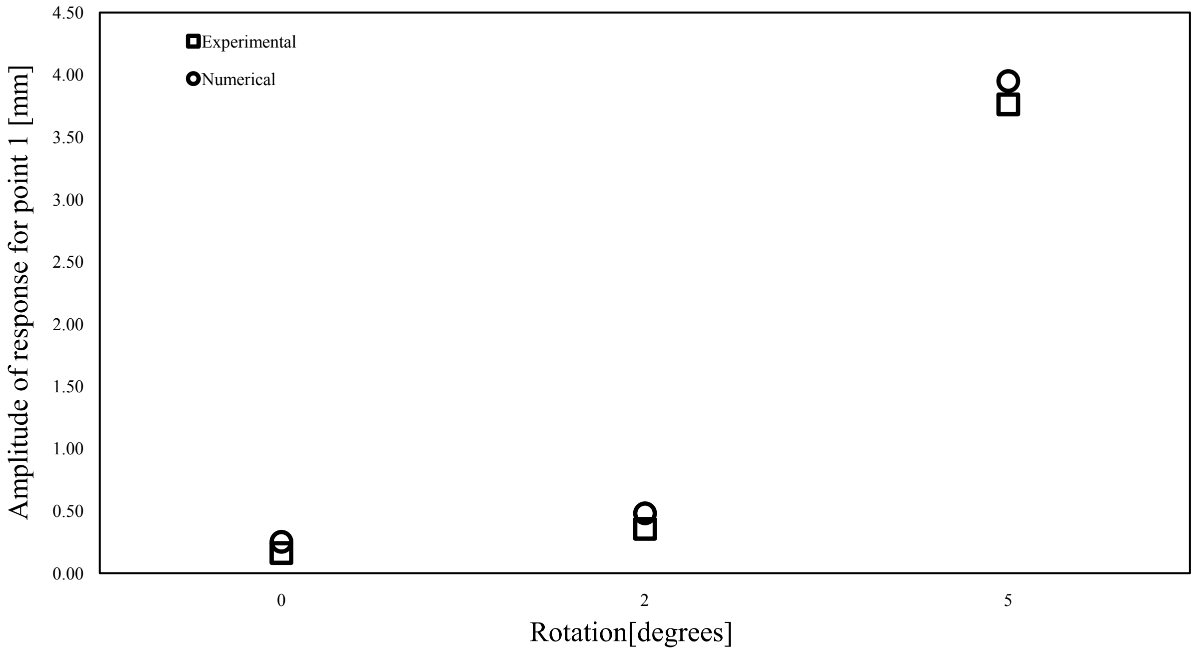

(a) Lateral response.

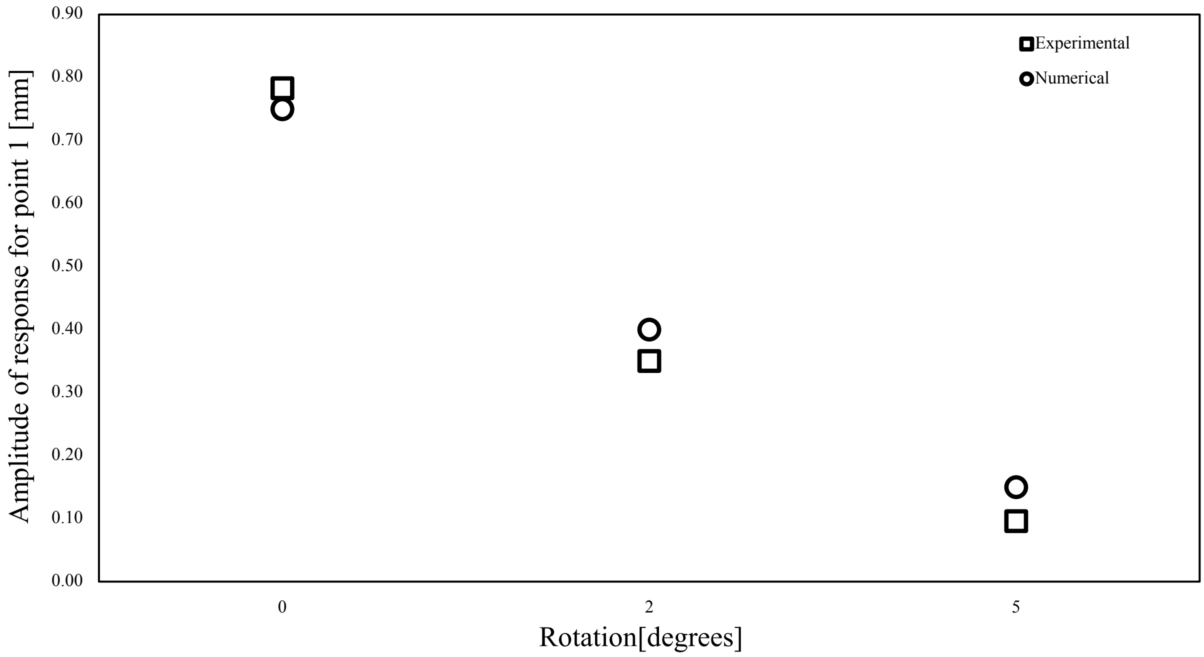

(b) Vertical response.

Figure 7.5: Rotation comparison (relative motion). Case: 7x1–4 mm–1 Hz–1 mm gap.

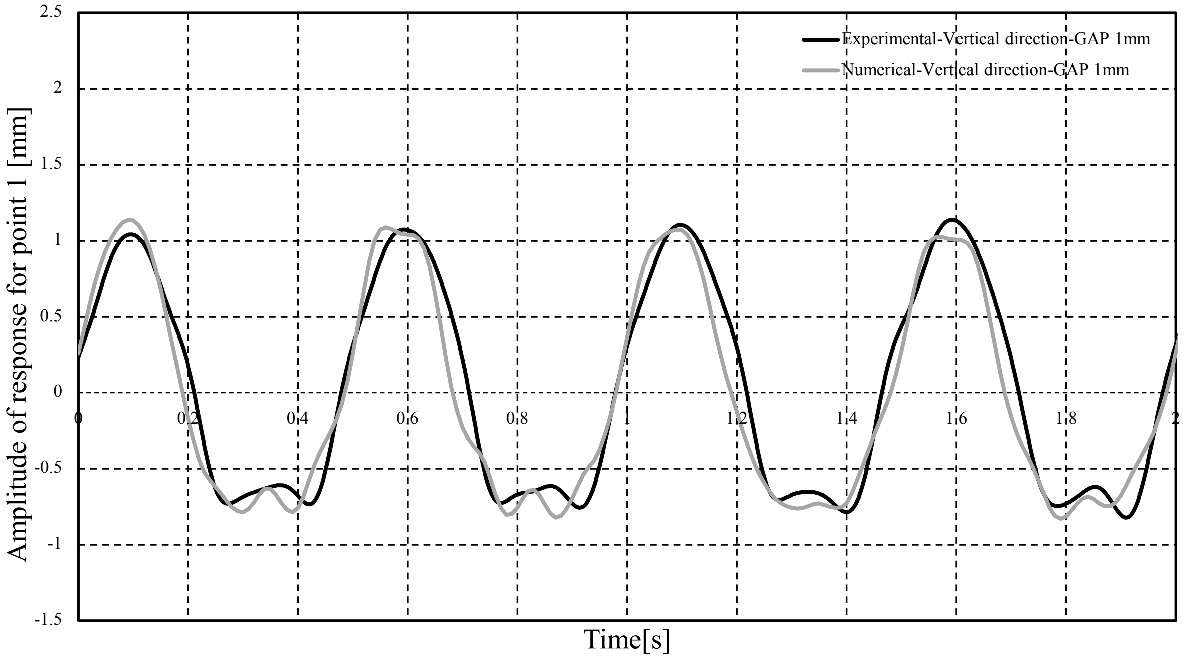

(a) 1 mm gap.

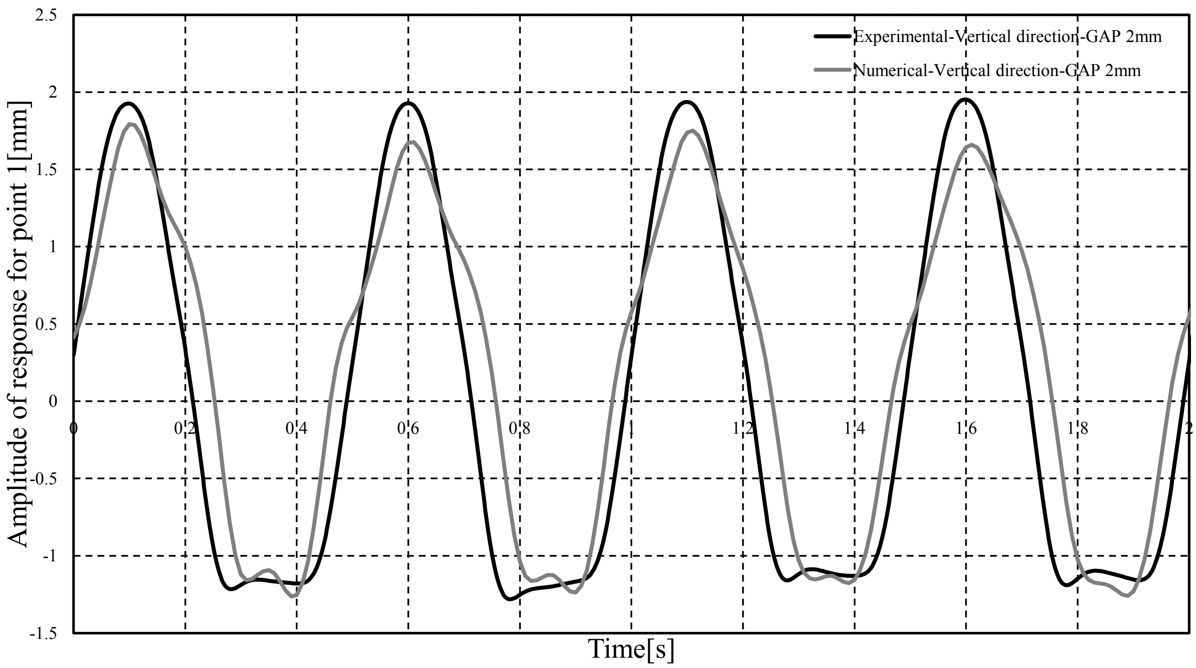

(b) 2 mm gap.

Figure 7.6: Gap size comparison (relative motion). Case: 7x1–2 Hz–0 degree–non loaded.

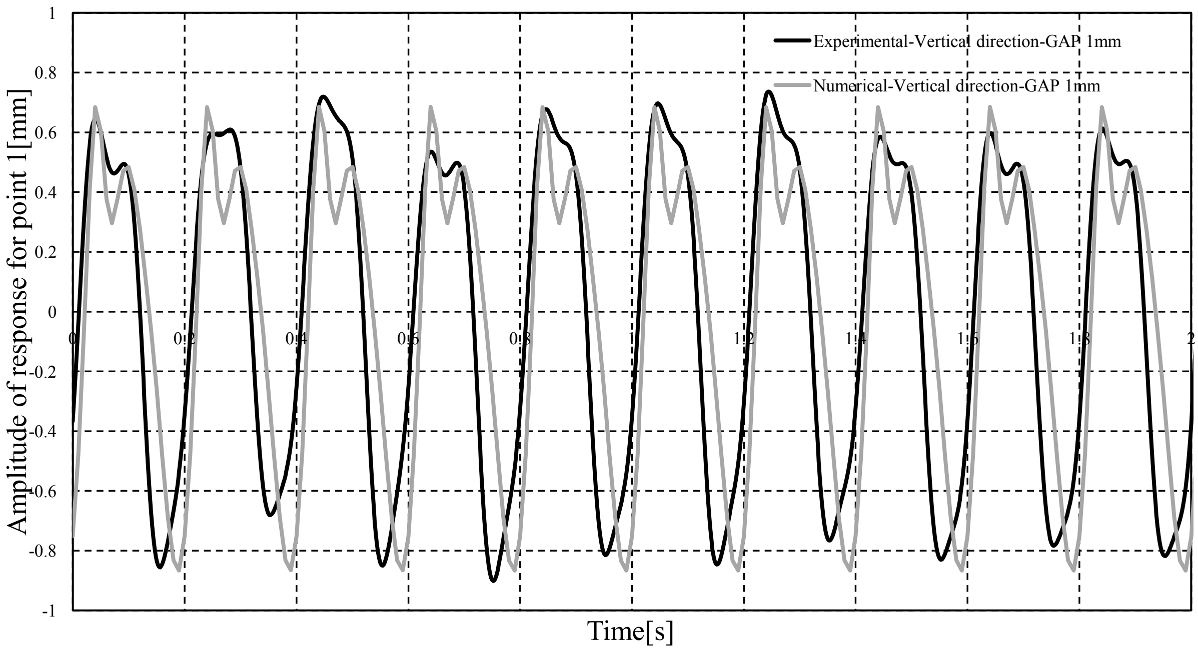

(a) 1 mm gap.

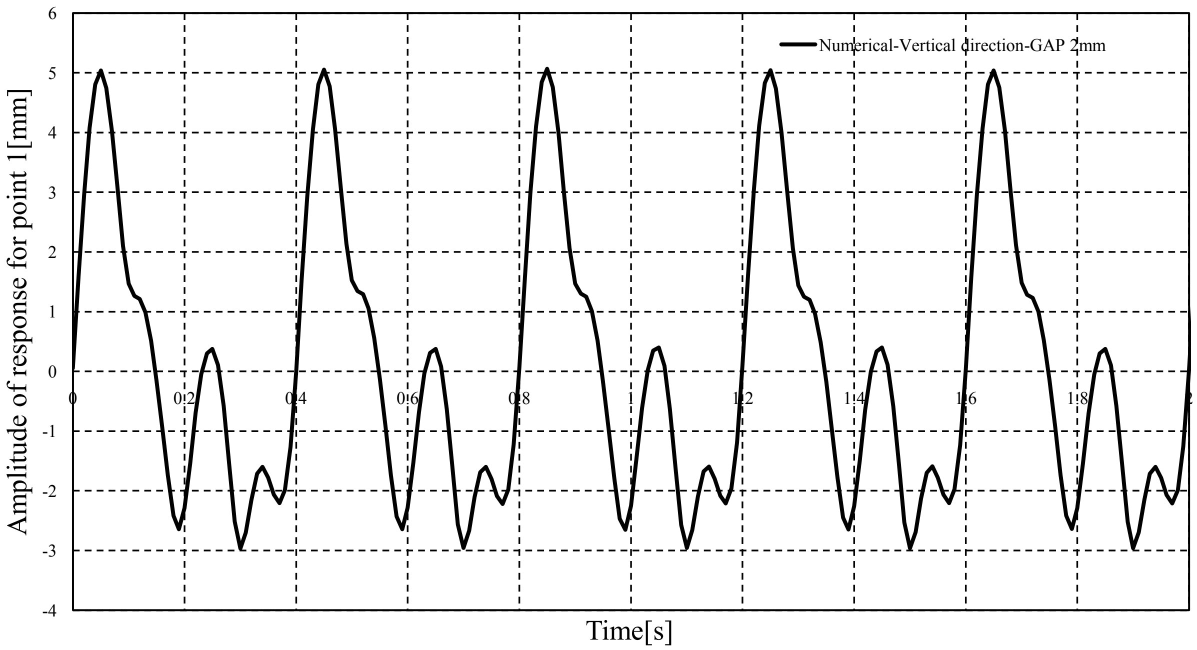

(b) 2 mm gap.

Figure 7.7: Gap size comparison (relative motion). Case: 7x1–5 Hz–0 degree–non loaded (there is no experimental data for 2 mm case).

The source of error in the experimental data may have its origin in the experiments' settings and is difficult to evaluate. As an example of experimental errors we observed three phenomena in the experimental data: significant lateral motion for the zero-degree cases, which is not observed in the numerical model, and pronounced bounce-back effect in 0.5 and 1 Hz frequency cases. Theoretically, this lateral response should be insignificant when compared to vertical response for the simple reason that there is no lateral component of driving excitation applied in this direction whatsoever. However, a significant response was measured in this direction as depicted in Figure 7.8. This intriguing lateral response is attributed to misalignments during containers placement, camera reflexive marker calibration and, as mentioned earlier small displacement amplitudes (2, 4 and 6 mm) applied to the system.

The second observation is that bounce-back effect is dependent on frequency because it is caused by radial force added to the gap non-linearity. Contrary to what was observed in the 2 and 5 Hz cases at low frequencies radial force is not the main component of force behind the bounce-back effect because it is too small in comparison to gravitational force acting on this system. Consequently, this effect should not be observed at 0.5 and 1 Hz. However, for low frequencies bounce-back effect was still present in numerical (non-pronounced) and experimental (pronounced effect) cases. Please see Figures 7.9a and 7.9b for details. Again these disparities are believed to have their origin in factors mentioned in the previous paragraph. Thus, it is our understanding that numerical data for this frequency range is more reliable than experimental data. Nonetheless, with rare exceptions, most analysis of the container stack dynamics is concentrated in 2 and 5 Hz cases.

The last observation regards the uncertainty regarding the driving frequency amplitude. In all cases a significant difference was observed in the amplitude measured and the theoretical amplitude that was expected to be applied in the system (Please refer to Figure 7.10a and 7.10b for details). These differences are attributed to the calibration of the reflexive marker area in previous trials, which induced a margin of error between 20% and 30% for lateral and vertical directions in some cases studied. Additionally, the the choice of very small values for the driving amplitude (2,4 and 6 mm) assisted the appearance of such discrepancies. Although the study involved a scaled model, amplitude values for the driving excitation should have been set in higher values to avoid this problem and even facilitate the filtering process, as mentioned in section: 2.6.

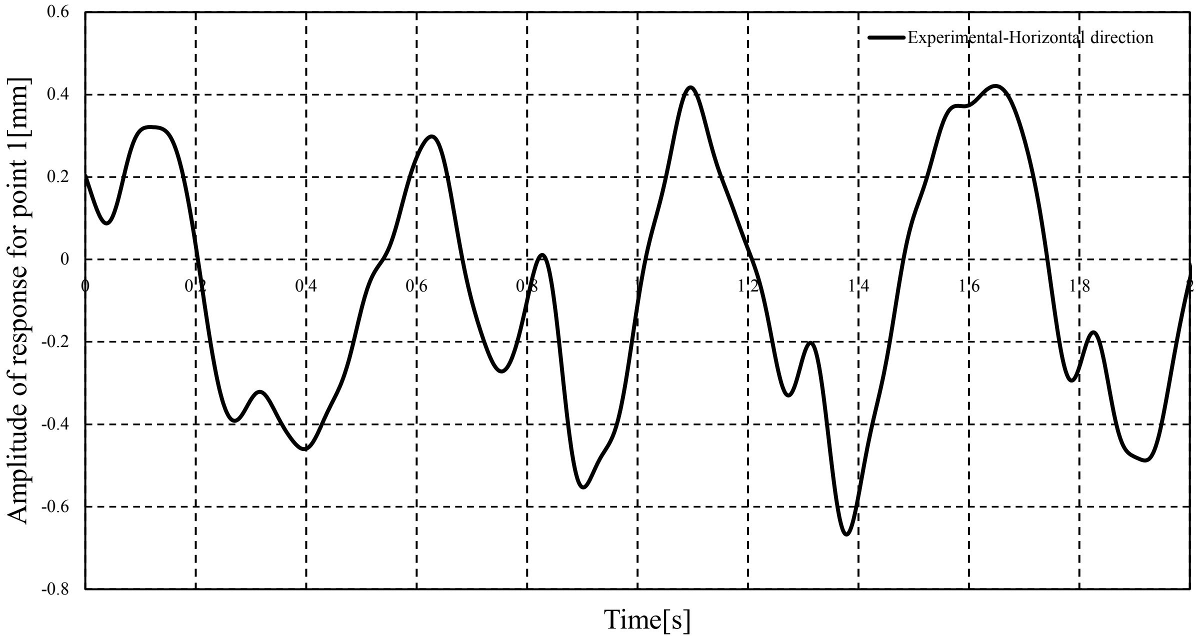

Figure 7.8: Local motion of point 1 in the lateral direction. Case: 7x1–6 mm–2 Hz–0 degree.

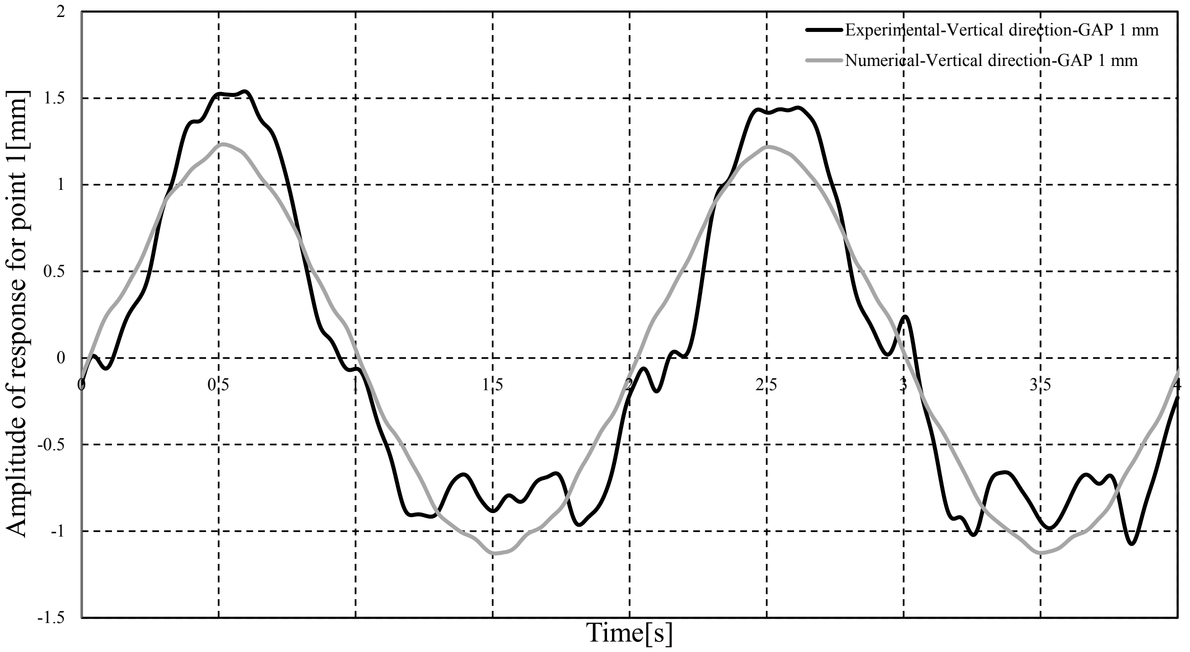

(a) Relative motion of point 1: frequency of 0.5 Hz, amplitude of 6 mm, no rotation, non-loaded.

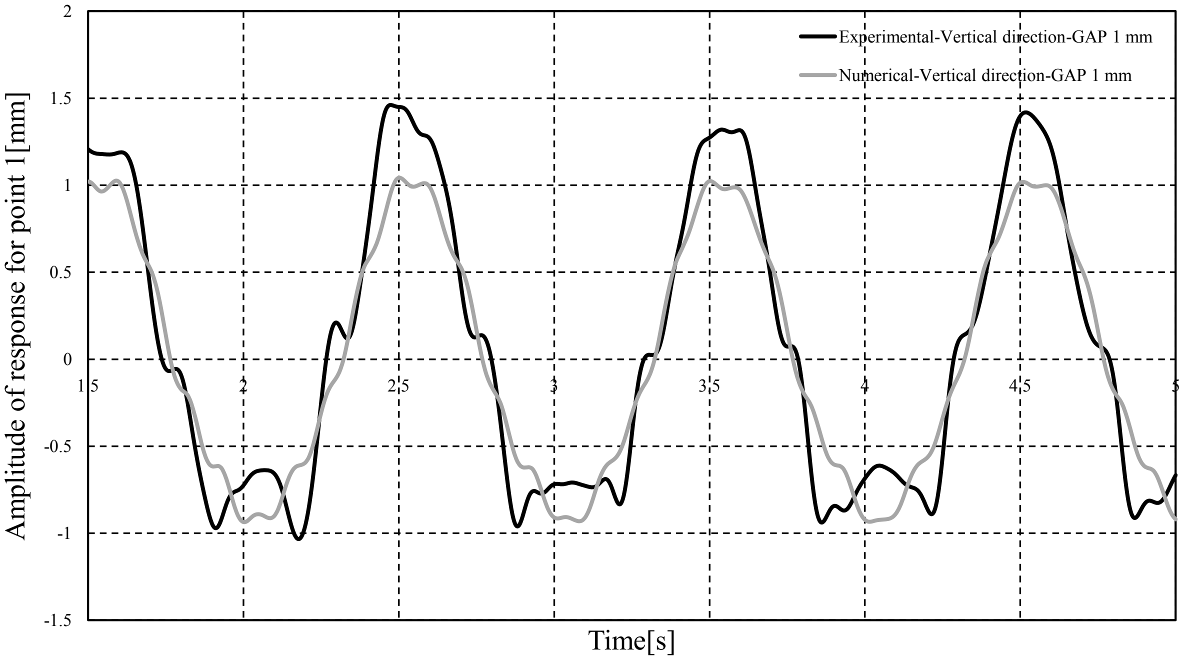

(b) Relative motion of point 1: frequency of 1 Hz, amplitude of 6 mm, no rotation, non-loaded.

Figure 7.9: Discrepancies for the response observed in point 1 (7x1).

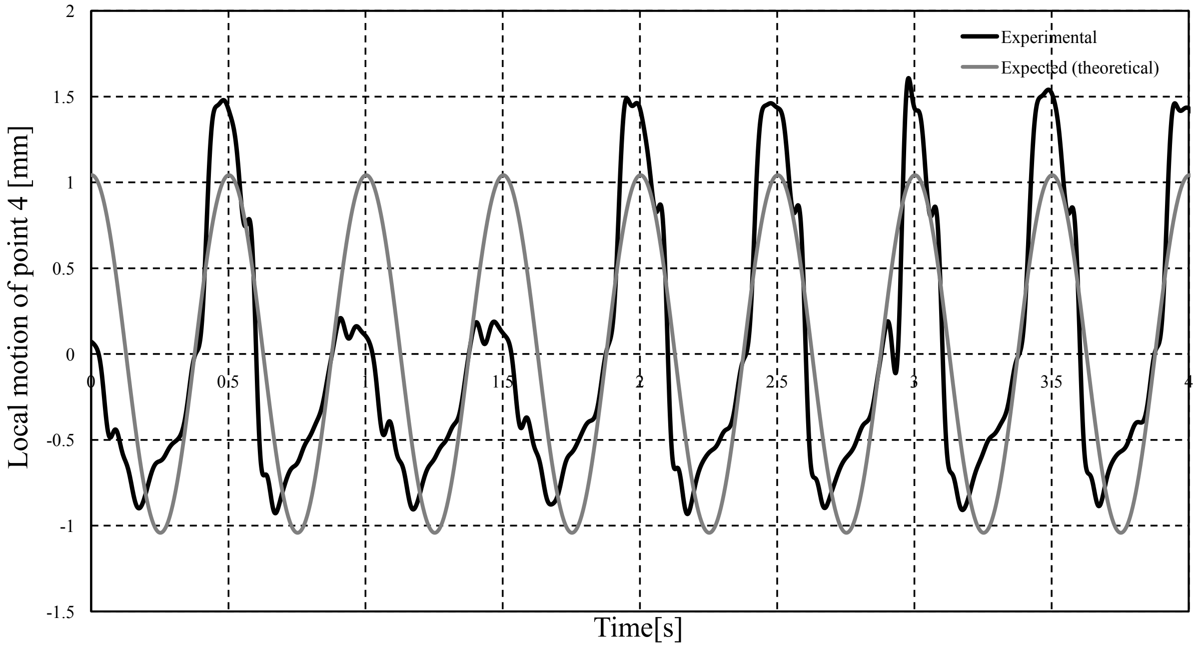

(a) Lateral direction.

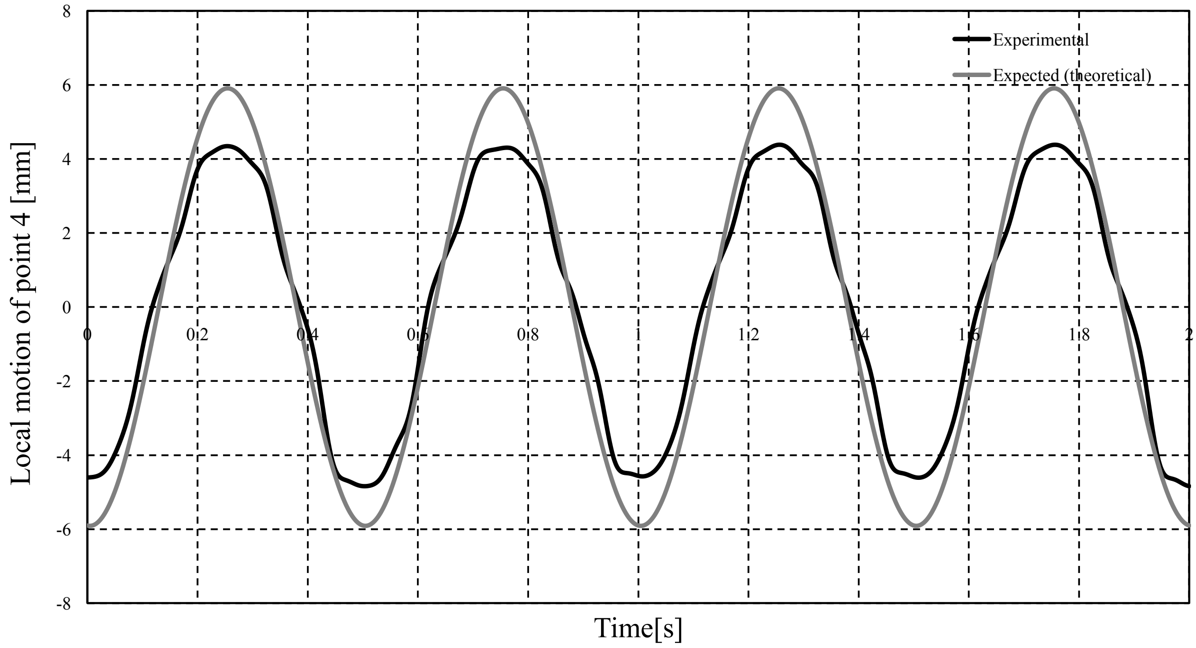

(b) Vertical direction.

Figure 7.10: Discrepancies for the driving excitation. Case: 7x1–6 mm–2 Hz–10 degrees.

7.2 Seven-tiers Three Stacks (7x3)

The study limited the analysis of displacement of a top corner of some individual containers. Furthermore, for means of comparison the highest container was used for evaluation purposes. In other words, points 1, 4, 5, 10 and 11 were used to analyze the mechanical behavior of the system. As mentioned in section 2.5, displacement-time response data was analyzed using three techniques: time history, coefficients of Fourier expansion and RMS value comparison.

7.2.1 Numerical Investigation: Finite Element Analysis (7x3)

A simplified 3-D finite element model of the system is as follows: twenty one scaled models of a 20 ft ISO freight dry container, twist locks and shaking table arranged in three stacks of seven-tiers. This model was developed using commercial software (Hypermesh 8.0, Altair Engineering Inc., 1995-2006). Details of the model's structure are presented in section 5.1. Scaled models were considered as steel frames sections compounded of circular and pipe beams (details of every profile are described in table 5.1). Numerical model is depicted in Figure 7.11. Moreover, twist locks were modeled using the mathematical relationship depicted in Figure 5.7.

Finally, the shaking table was considered a rigid body where the driving excitation follows same conditions imposed in the experiments (see table 4.3). Damping for the system was implemented using Rayleigh damping coefficients (see section 5.3.1) characterizing the main difference between this model and the model used during the pilot study. The numerical analysis was performed with a commercial finite element analysis package (Abaqus version 6.7, Dassault Systems), which accounts for geometry non-linearity considering a dynamic study in an implicit integration scheme.

Additionally, contact between adjacent containers was emulate using non-linear springs, placed on the corners castings considering only one degree of freedom (transversal/lateral direction). These contact forces, were calibrated through simple comparison between experimental and numerical data. The force elongation used for the contact forces is depicted in Figure 5.15b.

7.2.2 Numerical Model Validation (7x3)

Regarding the 7x3 cases, corresponding values for the experimental data were 0.28, 0.76, and 1.56 mm for the lateral direction, and 0.29, 0.36 and 0.46 mm for the vertical direction for the rotations of 0, 2 and 10 degrees, respectively. These measurements are consistent with some of the finite element prediction that were 0.0, 1.01 and 1.59 mm for the lateral

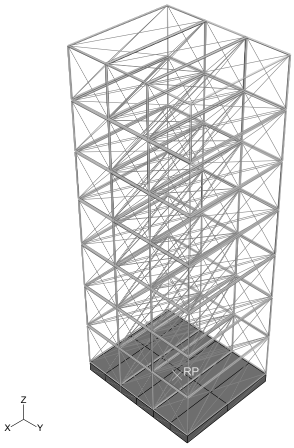

Figure 7.11: Finite element model of the seven-tier three stacks case (7x3).

direction and 0.29, 0.38 and 0.48 mm for the vertical direction for the respective rotation range. Differences between experimental and numerical data were 100%, 34.19% and 1.83% for the lateral direction. For the vertical direction these differences were 2.06%, 7.66% and 4.77%. Differences between each case can be clearly identified from time history comparison depicted in Figures 7.13, 7.14 and 7.15 for lateral and vertical responses.

Excluding the first case that presented a significant lateral component that is not present in the numerical model, differences between numerical and experimental results for the lateral and vertical direction are quite satisfactory. Lateral response discrepancy for the experimental data will be discussed in section 7.2.3. Regarding the effect of the only variable used for the 7x3 cases, rotation of the shaking table did not produced anything new. Lateral component of the response presents significant increase in point 1 (Figure 7.12a), which corroborates our understanding about the effect of this variable in the response. Inclining the container stack base favors the appearance of an extra lateral component of force (gravity force) besides the driving force, which helps the system to exceed the friction forces acting on the corner castings and consequently increase response. Following the same tendency, the vertical direction response increases with rotation also (Figure 7.12b).

7.2.3 Discrepancies (7x3)

Because of small sample size for the 7x3 study, it is impossible to perform an error estimative like it was conducted for the 7x1 cases. However, for the amplitude of the driving excitation some comments are necessary. In all cases a significant difference was observed in the amplitude measured and the theoretical amplitude that was expected to be applied in the system (Please refer to Figure 7.16a and 7.16b for details). These differences are

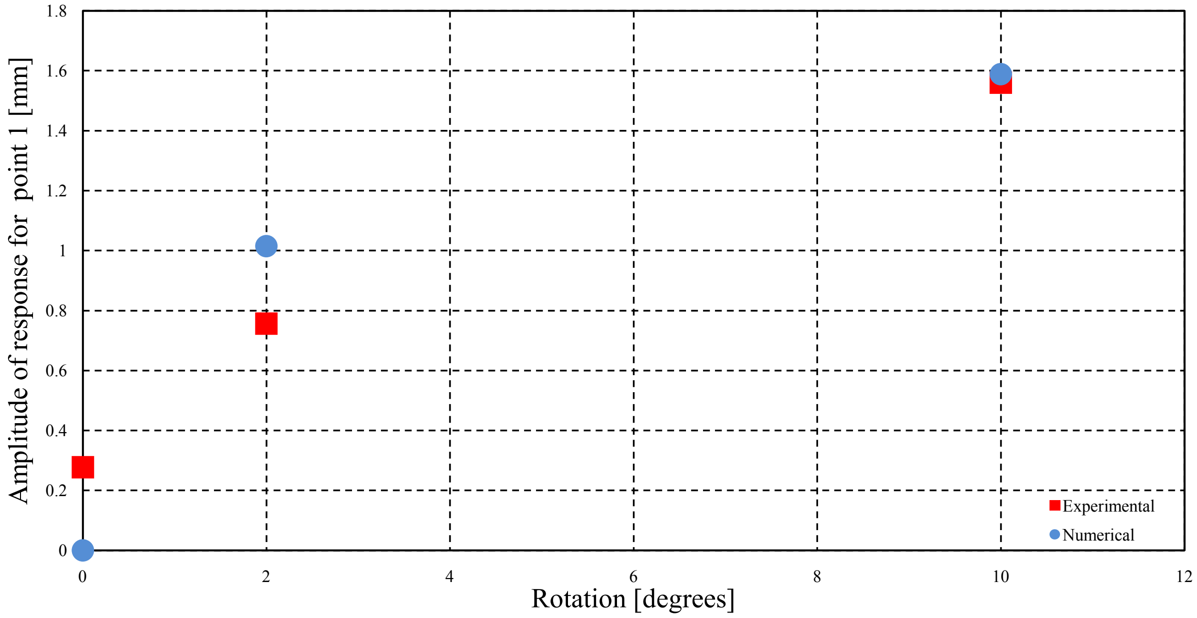

(a) Lateral response of point 1.

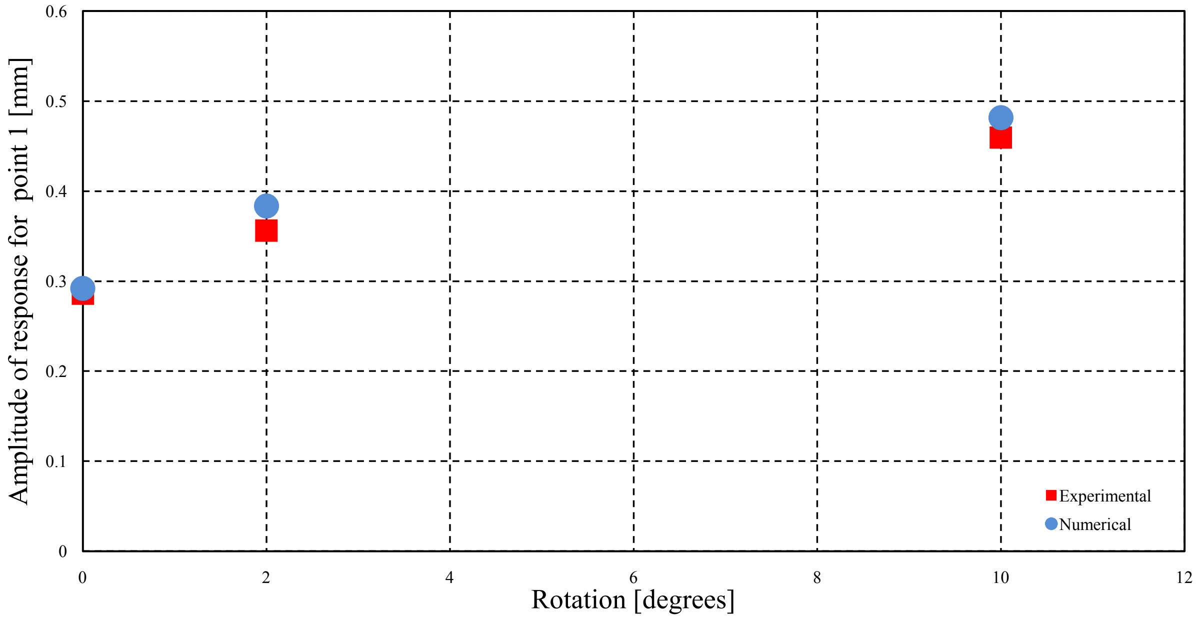

(b) Vertical response of point 1.

Figure 7.12: Rotation effect using RMS value comparison (relative motion). Case: 7x3–6 mm–2 Hz–1 mm gap–non loaded.

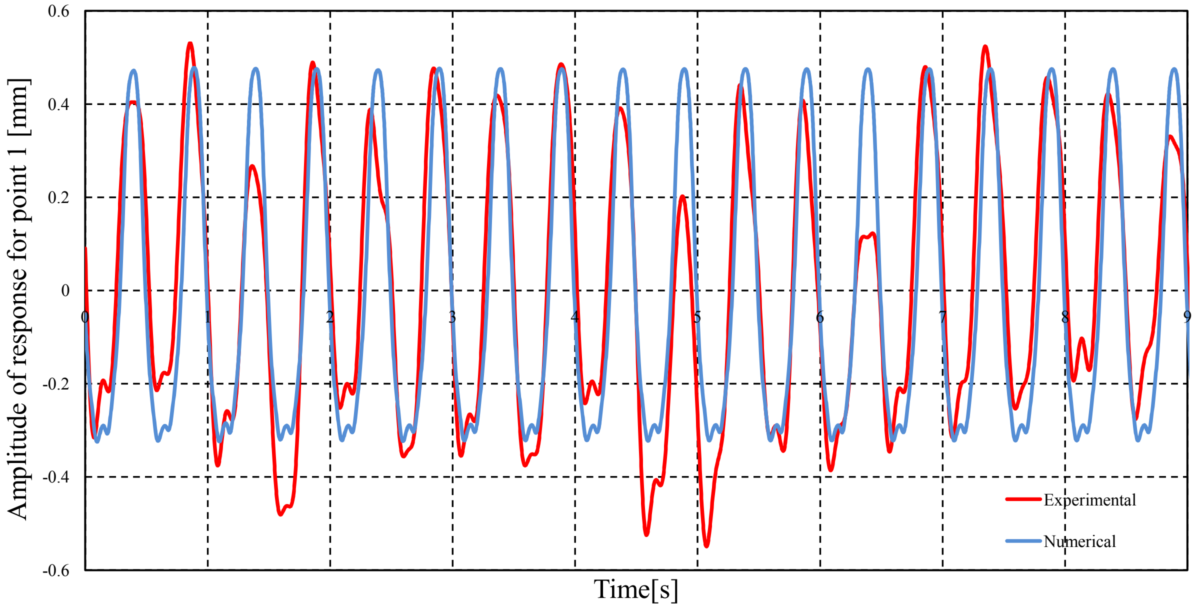

(a) Vertical response of point 1.

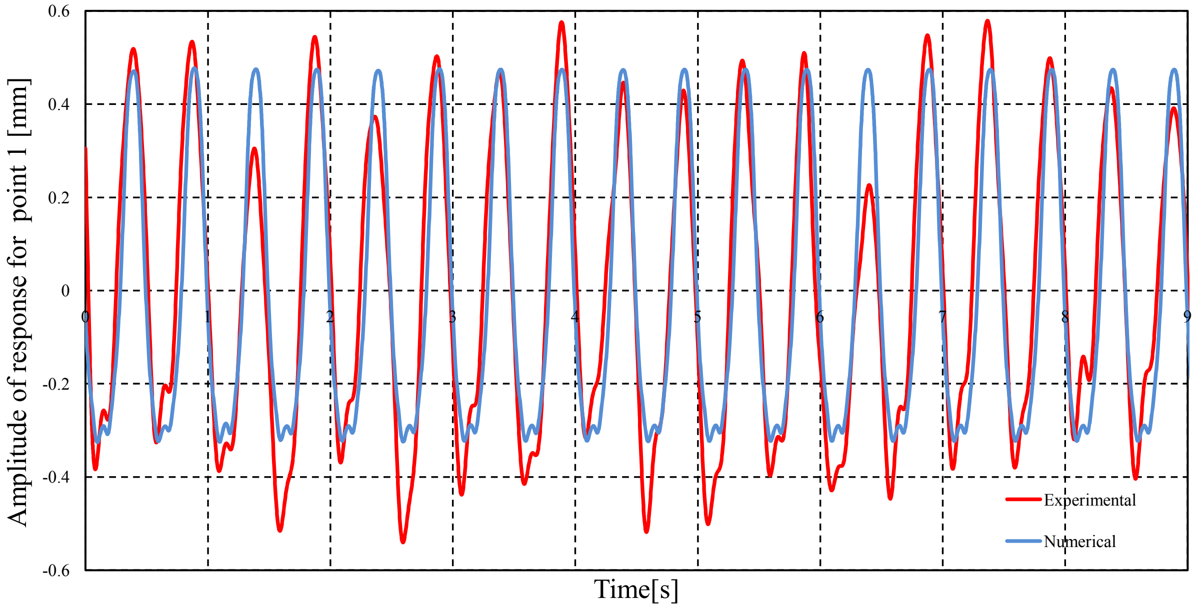

(b) Vertical response of point 5.

Figure 7.13: Comparison of numerical and experimental data (relative motion–7x3). Case: 7x3–6 mm–2 Hz–1 mm gap–0 degree–non loaded.

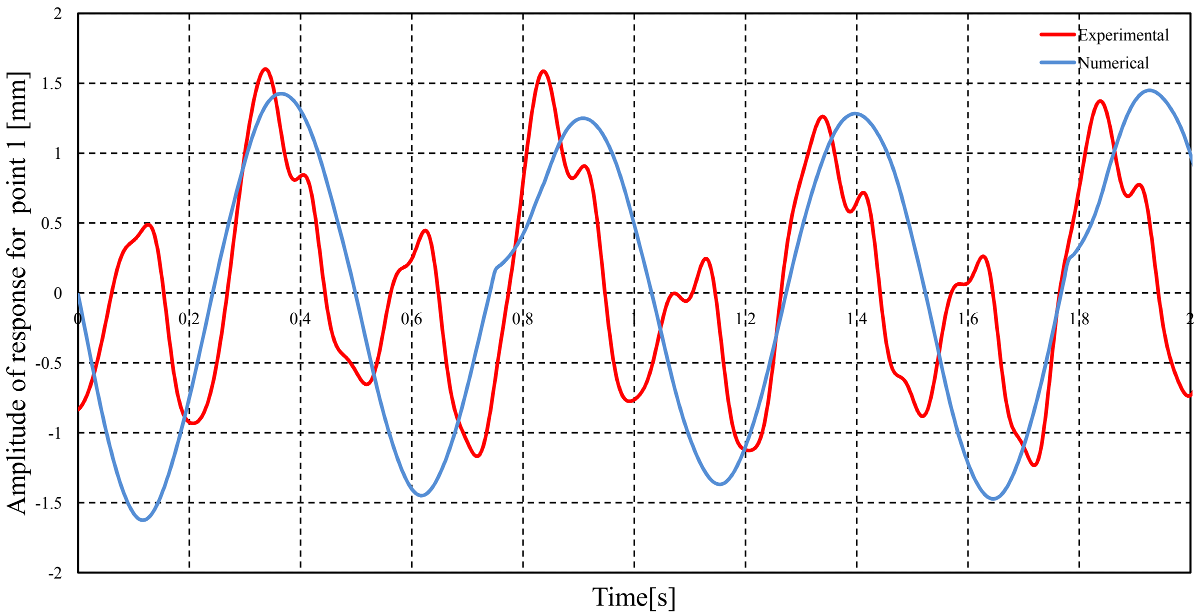

(a) Lateral response.

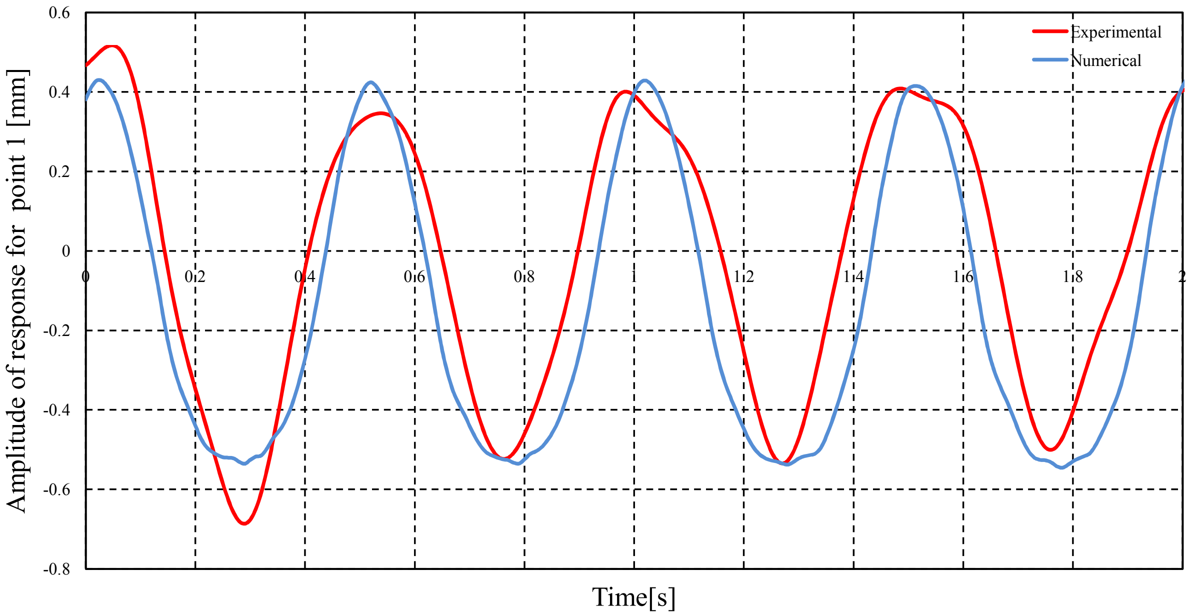

(b) Vertical response.

Figure 7.14: Comparison of numerical and experimental data (relative motion). Case: 7x3–6 mm–2 Hz–1 mm gap–2 degrees–non loaded.

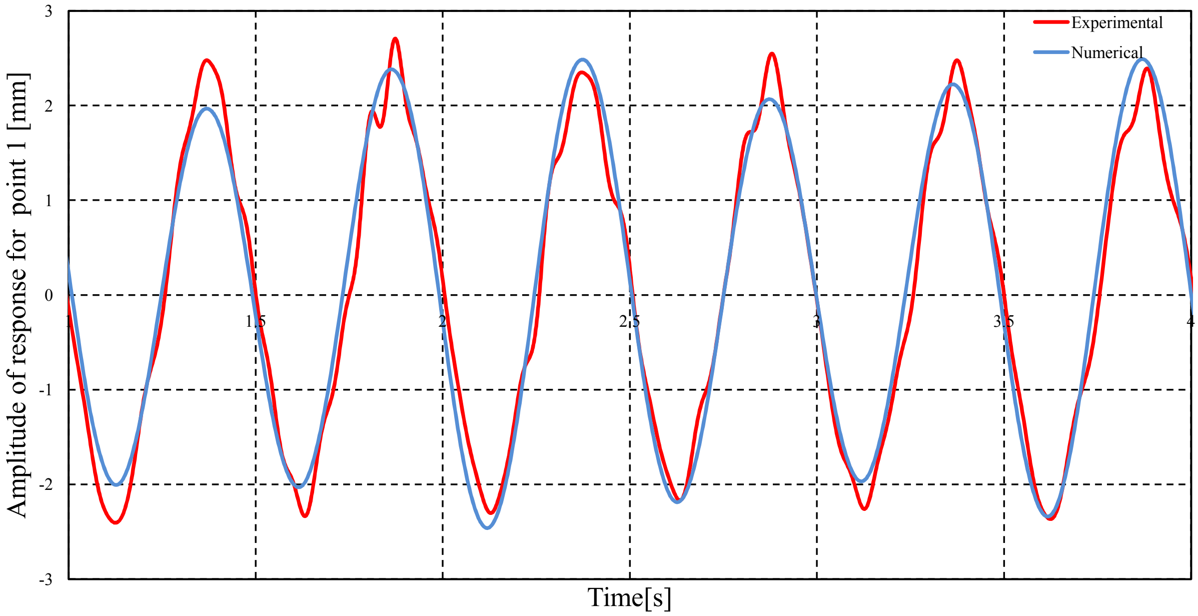

(a) Lateral response.

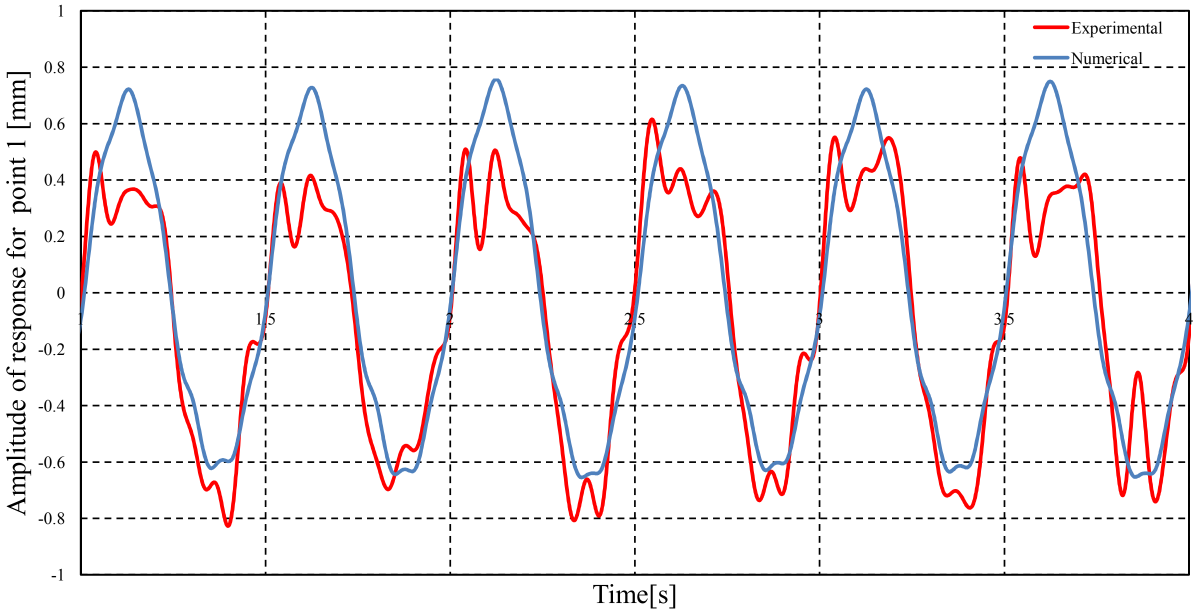

(b) Vertical response.

Figure 7.15: Comparison of numerical and experimental data (relative motion). Case: 7x3–6 mm–2 Hz–10 degrees–1 mm gap–non loaded.

attributed to the calibration of the reflexive marker area in previous trials and misalignments in the stack, which induced a margin of error around 20% for lateral and vertical directions in all the three cases studied. Additionally, in the case where lateral component is not supposed to be present a significant lateral response was measured, as can be seen in Figures 7.17a and 7.17b. Again this discrepancy is attributed to misalignments in the stack, which induce a lateral motion. Furthermore, contact between corner castings can move the contacting surfaces because of reaction which also can contribute for the lateral component.

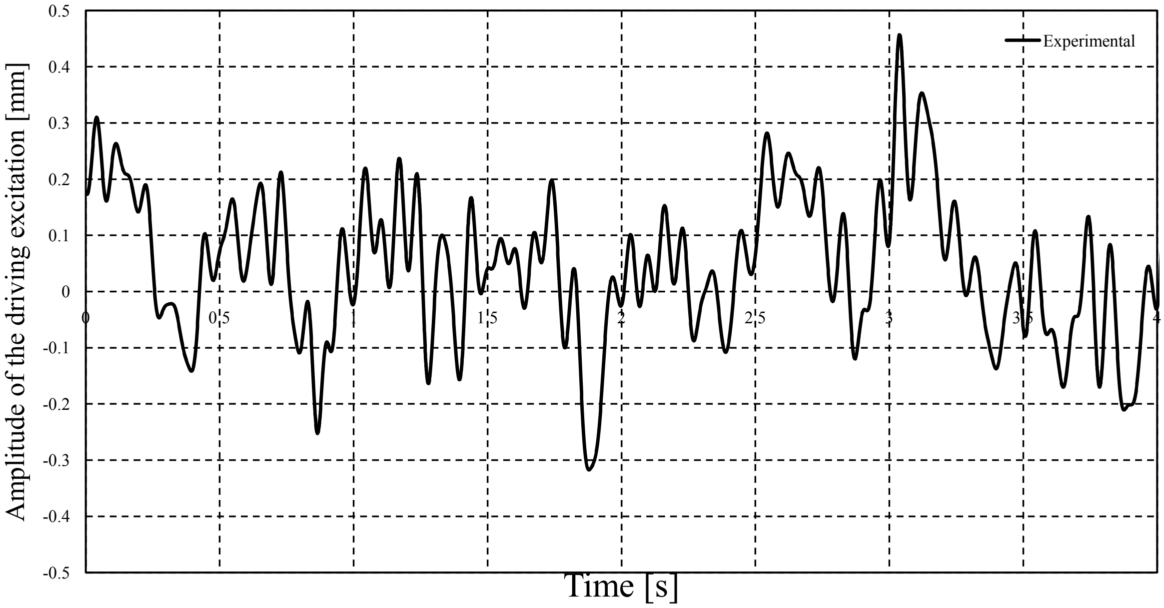

(a) Lateral direction.

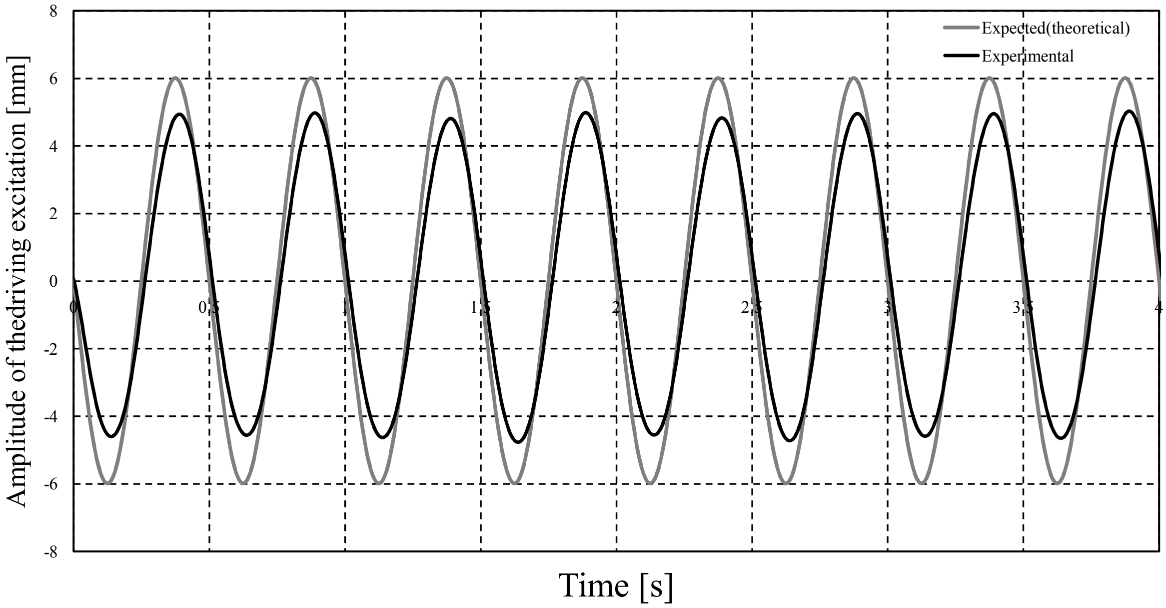

(b) Vertical direction.

Figure 7.16: Driving excitation discrepancy. Case: 7x3–6 mm–2 Hz–1 mm gap–0 degree–non loaded.

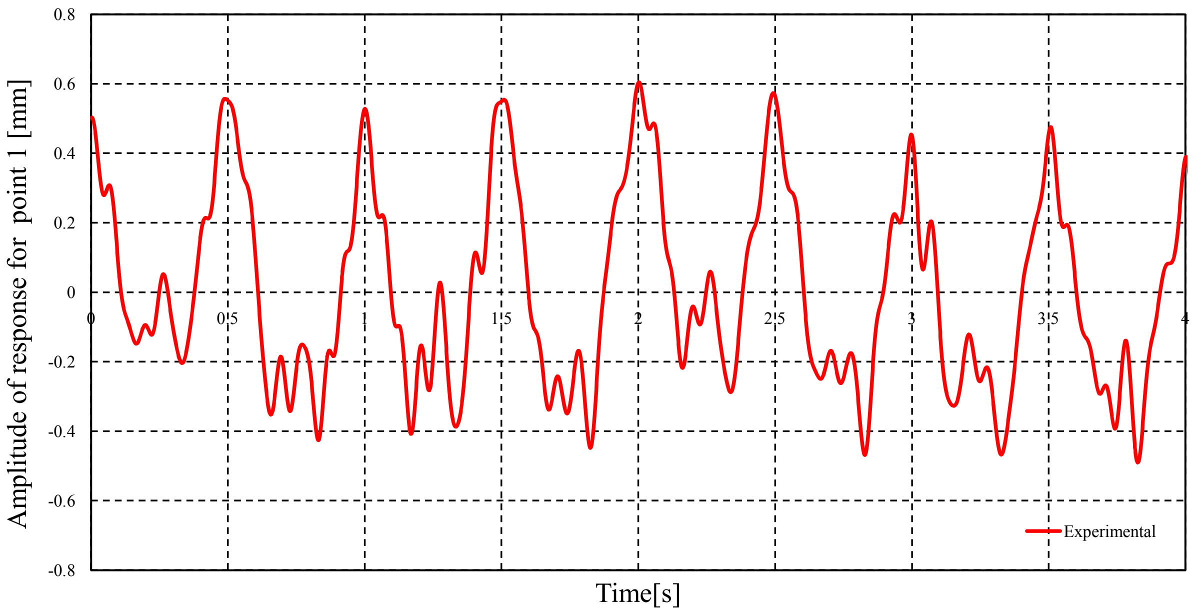

(a) Lateral direction.

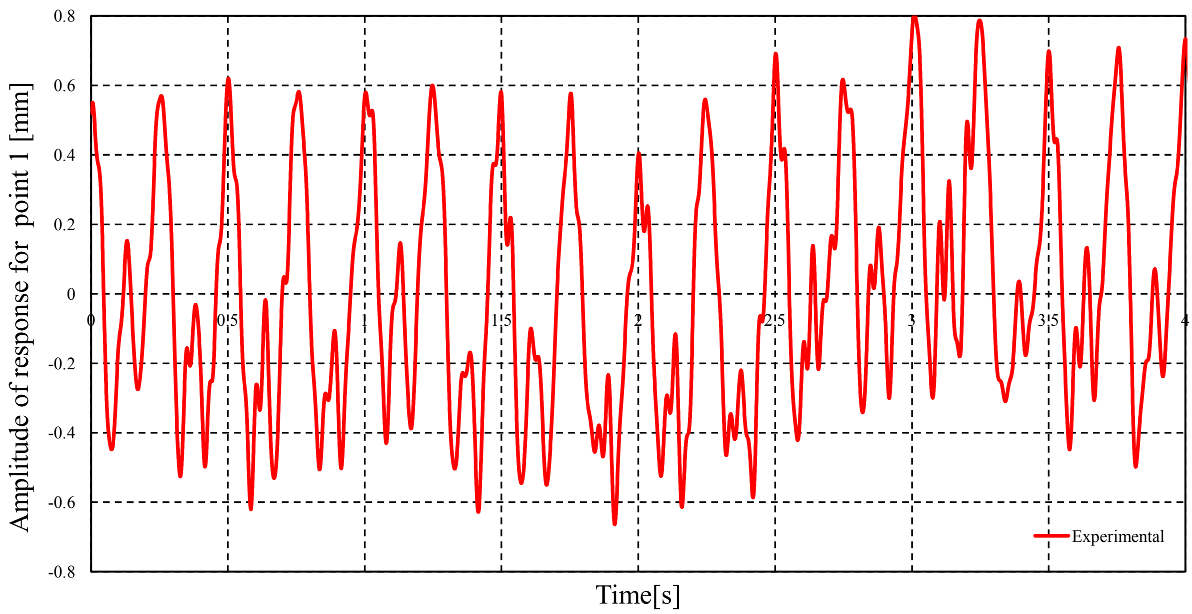

(b) Vertical direction.

Figure 7.17: Lateral displacement discrepancy. Case: 7x3–6 mm–2 Hz–1 mm gap–0 degree–non loaded.

Chapter 8

Simulation Results and Discussion

For the last section of this dissertation, numerical simulation was employed to identify important points in the container stack dynamics through input variables that it will be explained in each pertinent section. All of them are natural variables that are encountered during maritime transportation. Additionally, in order to evaluate the effect of changes in these input variables a more practical output variable is needed. Consequently, is the author intuition that force on the bottom twist locks (nonlinear springs) is a perfect choice. The reasoning behind is clear: securing systems, in particular, twist locks are responsible for container safety and the biggest contributor to the nonlinear behavior of container stacks. However, anything or near anything is known about its dynamical behavior during extreme conditions. In this panorama, monitoring its response to external excitation is a crucial step towards understanding the complex mechanisms behind containers securing systems failure.

Furthermore, this section will present some advice, based on numerical analysis, on how to minimize the effect of the variables on the bottom twist lock force using some simple measures that it will be addressed in the next section. In general, these measures are ordered according to its simplicity, i.e., the simpler they are, the further they will be introduced and discussed.

8.1 Predictions and Advice (7x1)

Two single changes in the system would have great effect in the response and force experienced in the bottom twist lock: a decrease of twist lock gap size and the inclusion of a damper among corner castings. Both measures will be explored in this section and in the next section as well.

8.1.1 Gap Effect on Heaving

A simple geometrical change in twist lock features would affect the response and the force greatly: decreasing gap size has as effect a significant decrease in the response and force, as can be seen in Figures 8.1a, 8.1b and 8.3a. This is a promising alternative to minimize the system's response and consequently force experienced by the twist locks. Even though changes in this variable have little tolerance for adjustment in real situations, it is something that should be considered because of its simplicity. It is important to emphasize that this variable has no correlation to frequency, i.e., changes in frequency do not affect the output of changes in gap size. This is one of the most important findings to emerge from this study. Considering the fact that container ships present different frequency ranges for every motion (pitching, rolling, heaving, etc.) this variable must be explored as a solution. As mentioned earlier the main limitation lies in the fact that changes in this variable can retard or even impair the linking process that actually is quite simple.

8.1.2 Damper Effect on Heaving

Another approach that can be used to decrease the dynamic response of the system is to incorporate energy dissipating mechanisms into it[23]. This can be achieved by various methods, e.g., high damping elastomeric bearings, lead plugs in elastomeric bearings, mild steel dampers, fluid viscous dampers, and friction in sliding. For a review about these systems please refer to Buckle [14], Kelly [42] and Soong [74]. In our case, the second change that was implemented was the inclusion of a viscous damper (velocity-dependent) in twist locks' original geometry. This is a relatively simple change in just one of the linking components. This change presents a significant decrease in response, an effect depicted in Figures 8.2a, 8.2b and 8.3b. However, the authors have no knowledge about the feasibility of this change, which could impact companies' costs and bring uncertainty about operational time. Additionally, some authors like Hanson [33] and Kelly [43] adverted that increasing the viscous damping has a significant effect on the dynamic response of the system only when the excitation frequency is nearly the same as the natural frequency of the system or within a 20% range from this value. In other words, effectiveness of dampers are highly frequency dependent, which can be another important limitation for practical applications, keeping in mind that ship's motion, even when coupled, have distinct frequencies ranges.

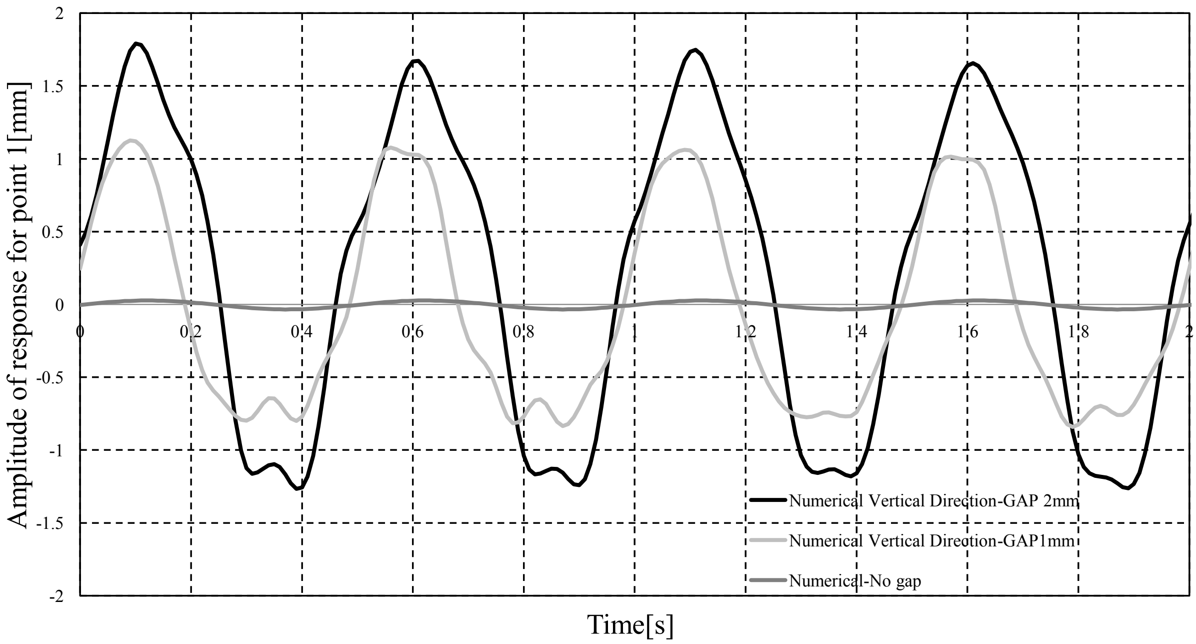

(a) 2 Hz (relative motion).

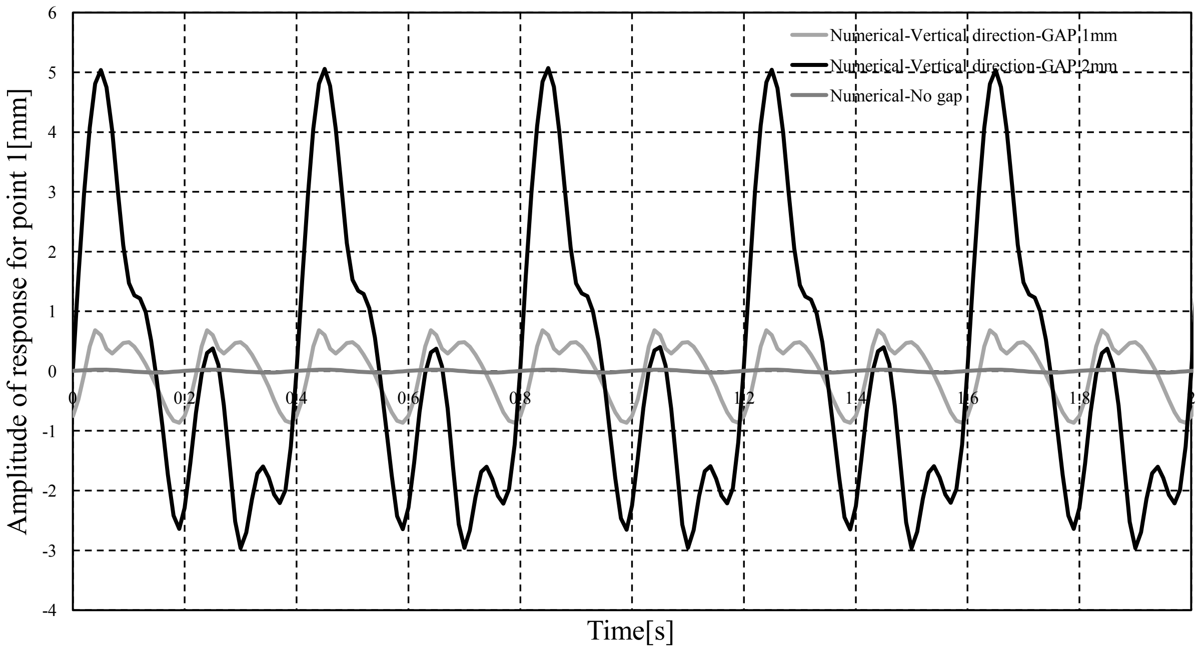

(b) 5 Hz (relative motion).

Figure 8.1: Effect of decreasing the gap size on heaving. Case: 7x1–6 mm–1 mm gap–0 degree–non loaded.

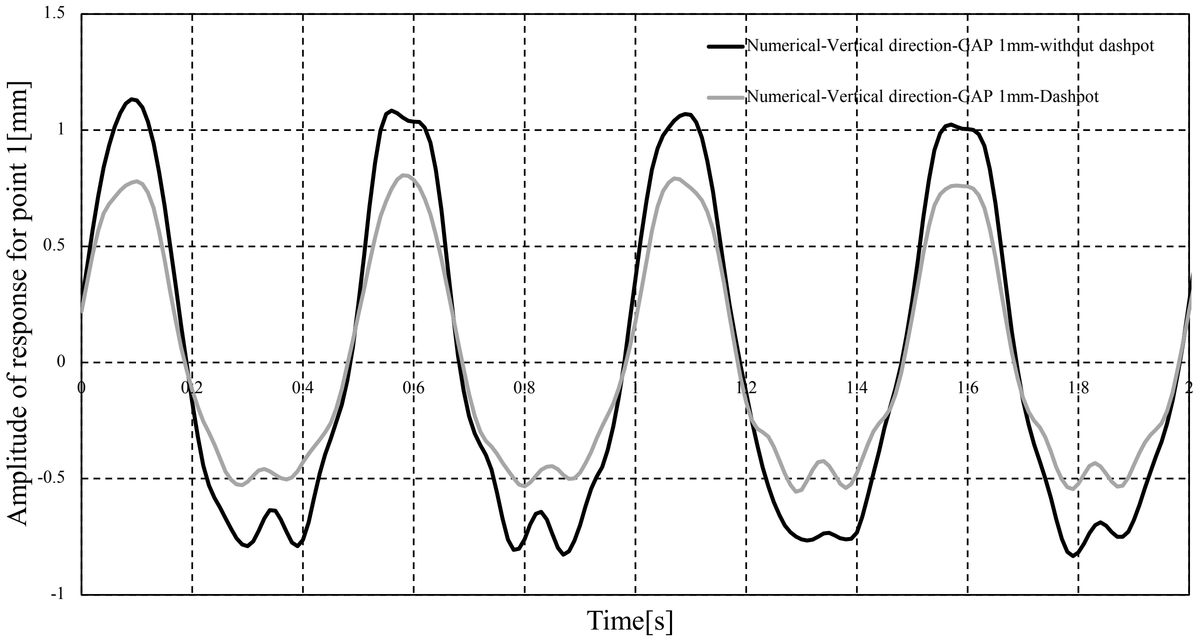

(a) Frequency 2 Hz.

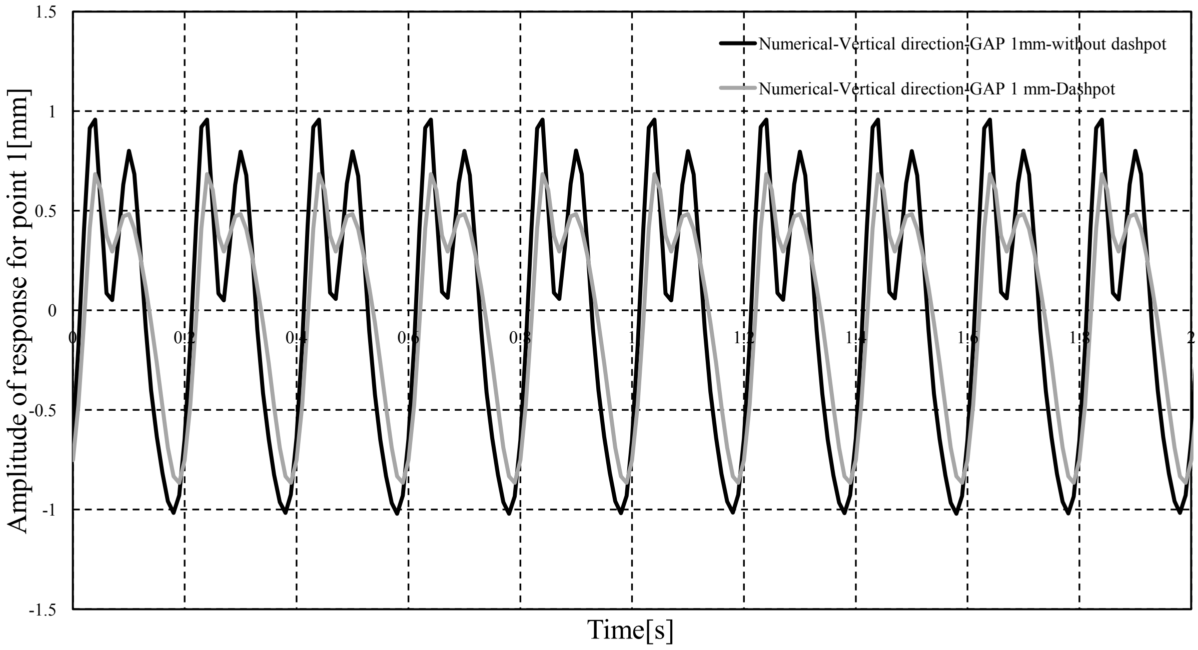

(b) Frequency 5 Hz.

Figure 8.2: Effectiveness of dampers–Dashpot effect. Case: 7x1–6 mm–1 mm gap–0 degree–non loaded.

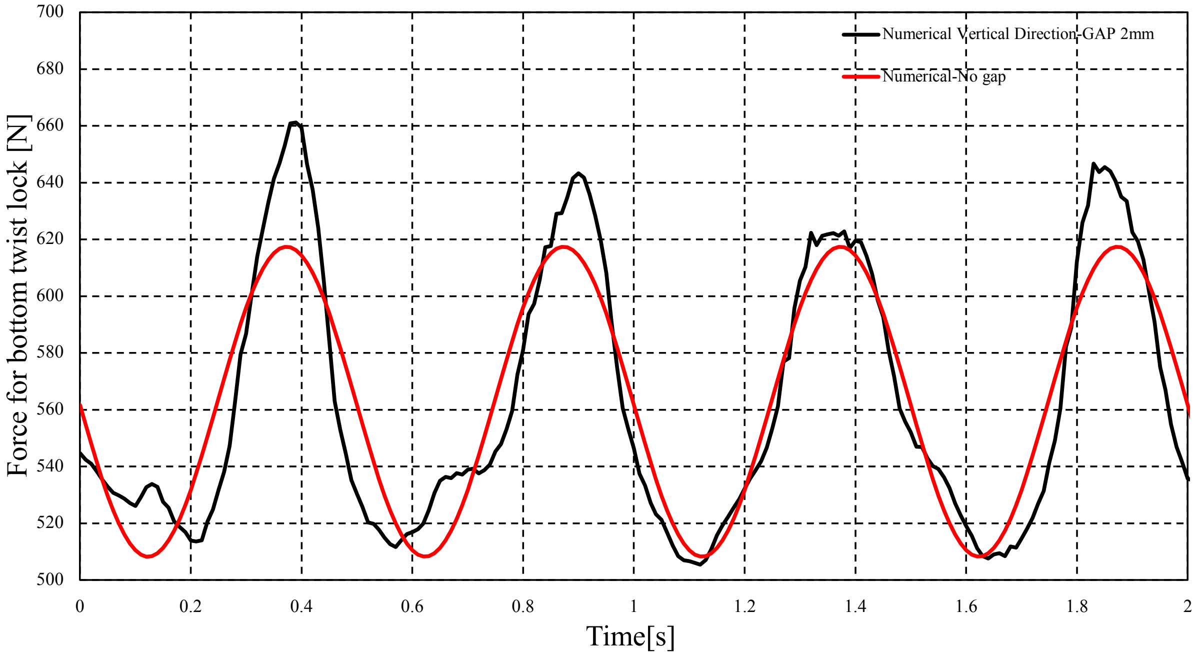

(a) Gap effect.

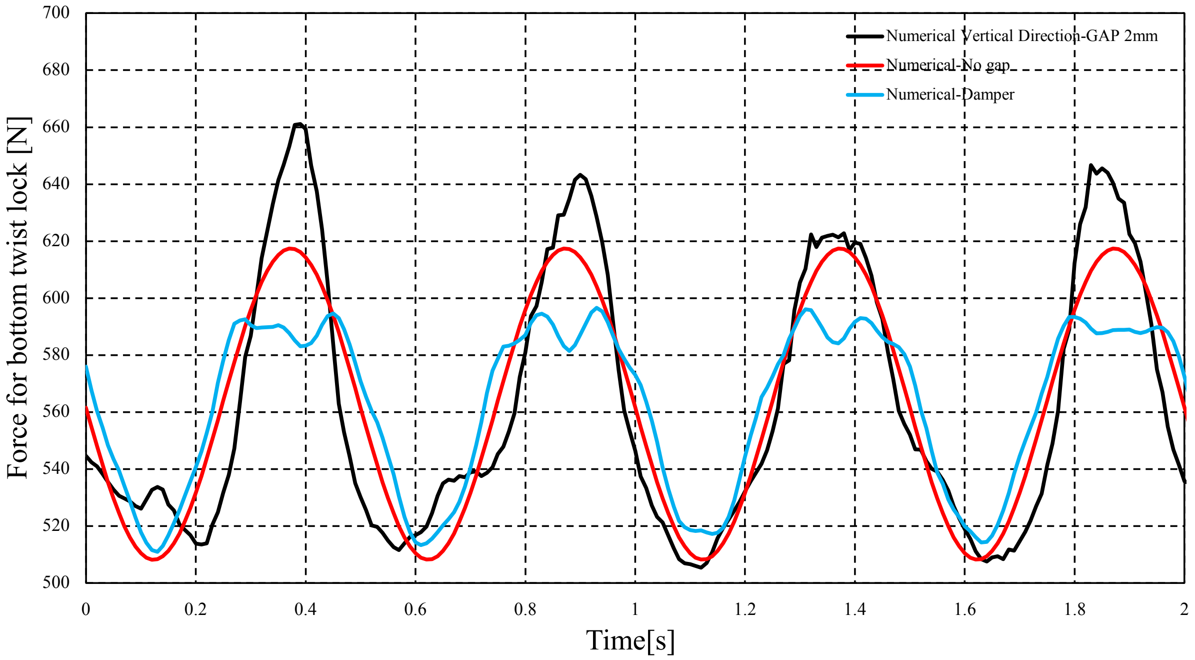

(b) Damper effect.

Figure 8.3: Changes in force caused by decrease in gap size and inclusion of a damper. Case: 7x1–6 mm–2 Hz–1 mm gap–0 degree–non loaded.

8.1.3 Payload Effect on Heaving

Besides these two changes, another two simple measures can be employed: changes in container stiffness and proper payload distribution. Although the concept is not new, it is important to emphasize that proper payload distribution is important to keep the stack response to a minimum. As can be observed in Figure 8.4, the allocation of a container at its full capability affects greatly the relative motion of point 1 and the force in the bottom twist lock. From the same figure it can be seen also that the higher the position of a fully loaded container in the stack, the higher the response, which can contribute greatly to the stress experienced by the whole securing system. Another factor to be emphasize is the fact that the force experienced by the bottom twist lock becomes non-linear with the raise of the payload in the stack, i.e., the higher the position of the payload, the higher the non-linearity observed. This phenomenon is observed in Figure 8.4b, and it is attributed to the gap. This is another interesting finding to emerge in the study: non-linearities observed seem to have a relation with payload distribution in the stack. Furthermore, a poor payload distribution can affect the ship's stability, so it is important to maintain the heaviest containers in low tiers.

8.1.4 Stiffness Effect on Heaving

Changes in container stiffness must be addressed with extreme caution. Normal and transverse forces induced by a ship's motion and wind loads in a container stack have their effects minimized through two physical phenomena: resistance from the lashing system, and absorption from the container structure itself. Additionally, the fact that the front and back of a container have different stiffness contributes to increase the complexity of the problem. In general, the open end (back) is more elastic than the closed end (back), which obligates calculations to be performed for door and front ends. Thus, to decrease the complexity of the problem, stage lashing system will not be taken into account for this analysis. The study will concentrate on the effect of changes in stiffness of the closed end for an inclined case (10 degrees), which it will naturally present both normal and transverse components. This side was chosen because the highest racking loads are located here due to its more rigid structure.

This study has found that changes in a structure stiffness has a direct impact in the structural response and force, as can be observed in Figures 8.5, 8.6 and 8.7. However, the system responds distinctly to increases and decreases in racking stiffness (Please refer to Figures 8.6a and 8.6b). In other words, an increase in the racking stiffness seems to have an effect on the response for both directions. However, decrease has a very limited effect.

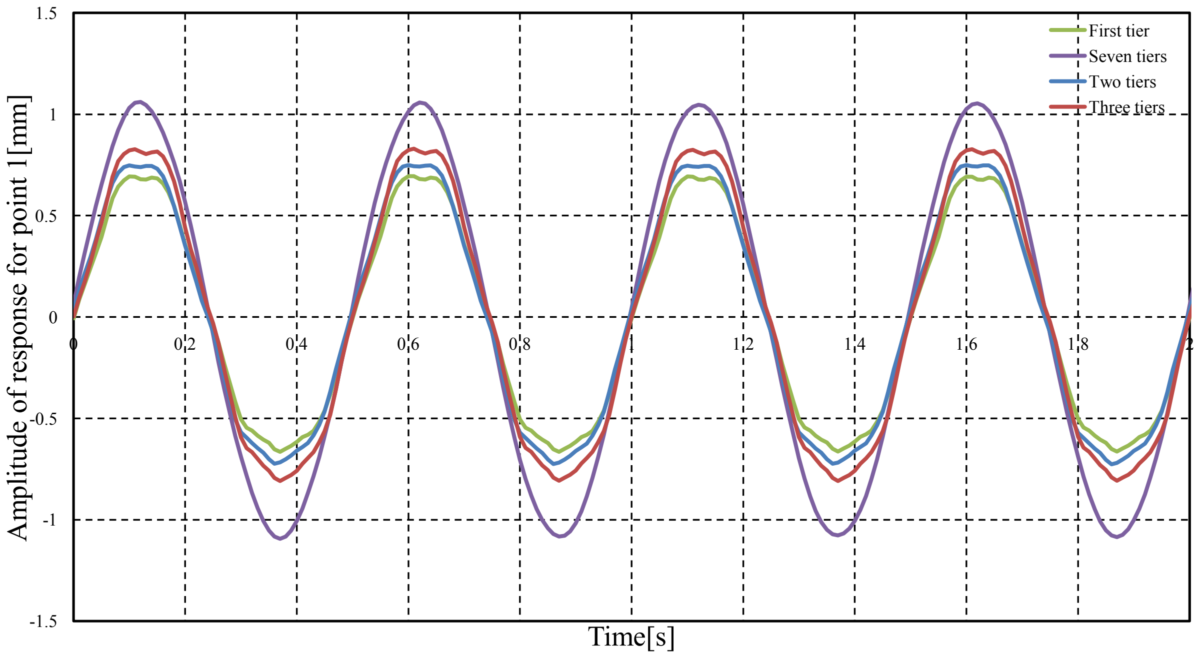

(a) Displacement of point 1 (relative motion).

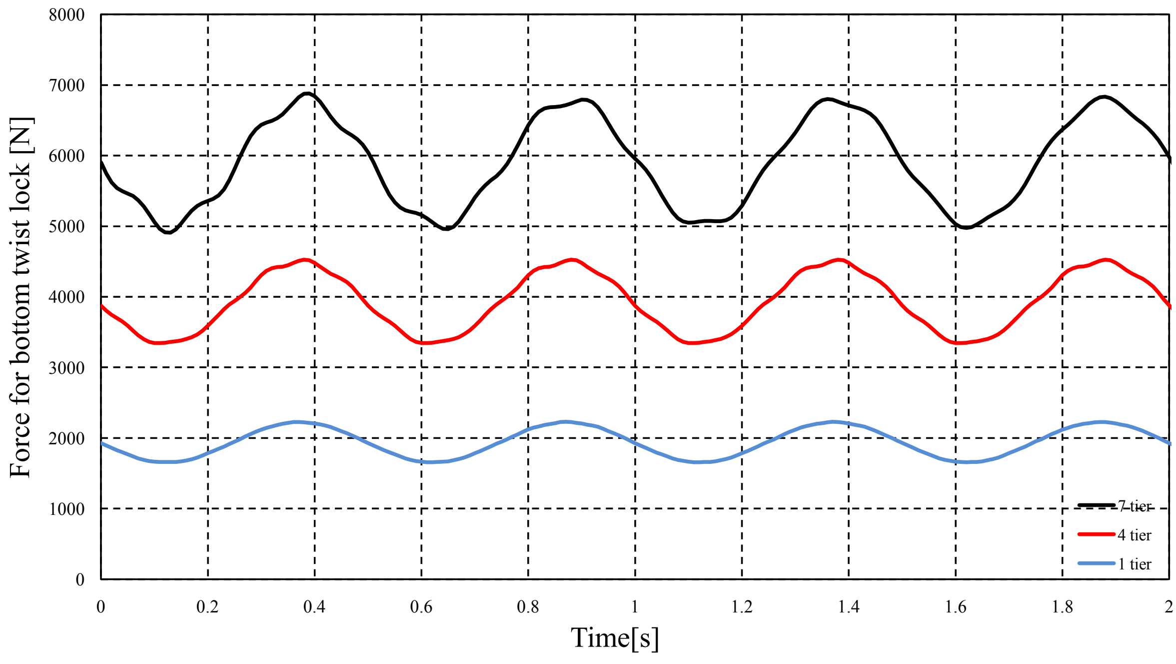

(b) Force on the bottom twist lock.

Figure 8.4: Effect of payload position in the tiers. Case: 7x1–6 mm–2 Hz–1 mm gap–0 degree.

Considering increase: for the lateral direction, an increase in stiffness causes a decrease in the response (17%). At the same time an increase is observed in the RMS value for the force (12.5%) of the bottom twist lock. However, this case still presents maximum values close to the standard stiffness case. On the other hand, for the vertical direction, an increase in stiffness has a positive effect in the response, i.e., it induces an increase in the response (38%). For the the force the effect is similar: the increase in stiffness caused an increase of 5.07%. Although these findings are interesting, the findings should be used with extreme caution because the structure behaves differently for each direction. It is well known that the stiffer the container, the greater the load absorbed by it as pointed out by [27]. Thus, a more rigid container would induce a higher load absorption, which can lead the structure to a process of mechanical failure earlier than expected. Moreover, the vertical direction presented an increase in the response, which would necessarily require a redesign of the other elements in the securing system. Such changes would represent a considerable cost and time for companies.

Regarding decrease: for the lateral direction, a decrease in stiffness produced no significant effect on the response (less than 1%). The same was observed for the response in the vertical direction (3%). Force components for lateral and vertical directions were non-significant also: 1% and 1.1%, respectively. Consequently, the results of this investigation show that changes in the container standard structural stiffness would not contribute solving the problem of container loss. These results should not be considered separately, but rather as part of a more complex study involving more securing components (lashing bars).

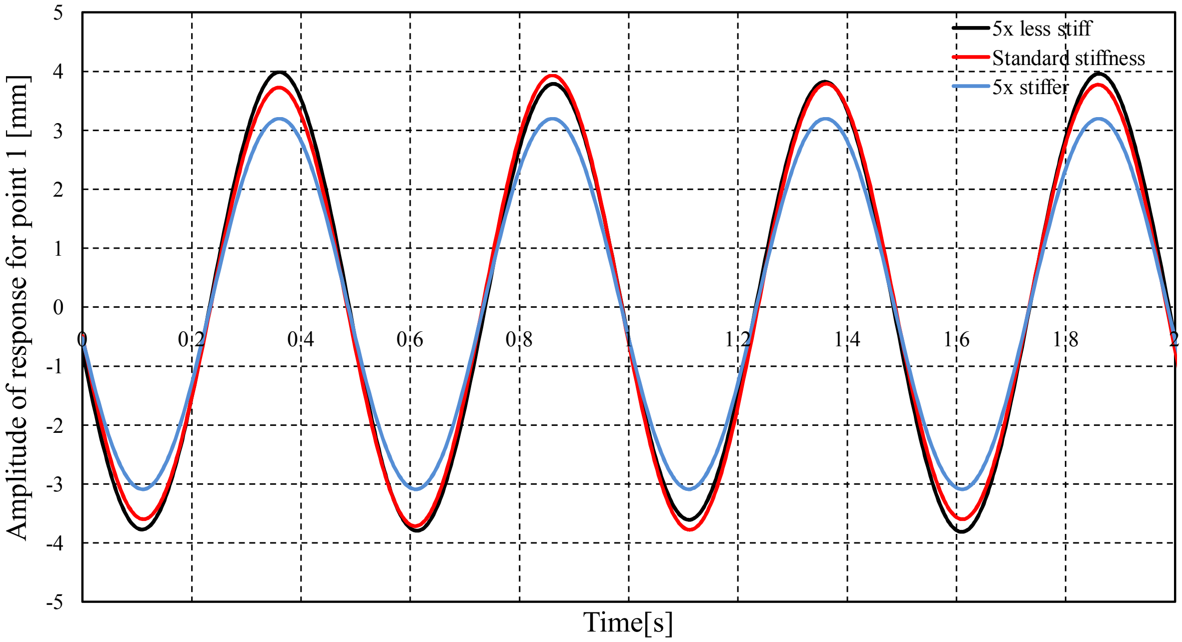

(a) Lateral direction.

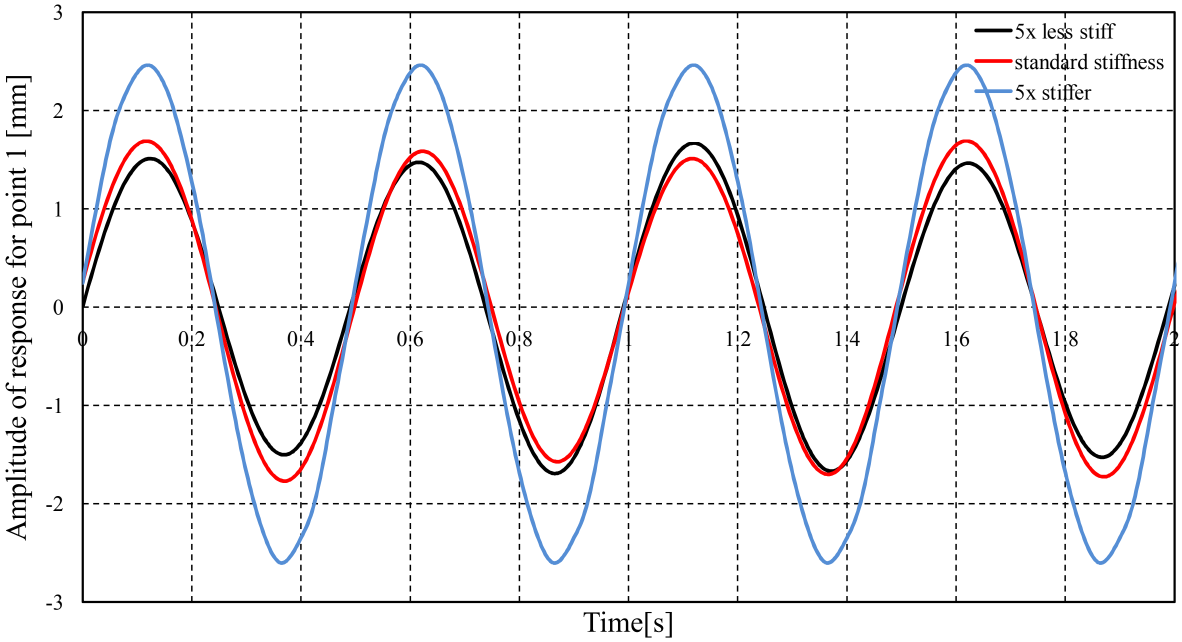

(b) Vertical direction.

Figure 8.5: Effect of changes in racking stiffness on the relative motion of point 1 (time history comparison). Case: 7x1–6 mm–2 Hz–10 degrees–non loaded.

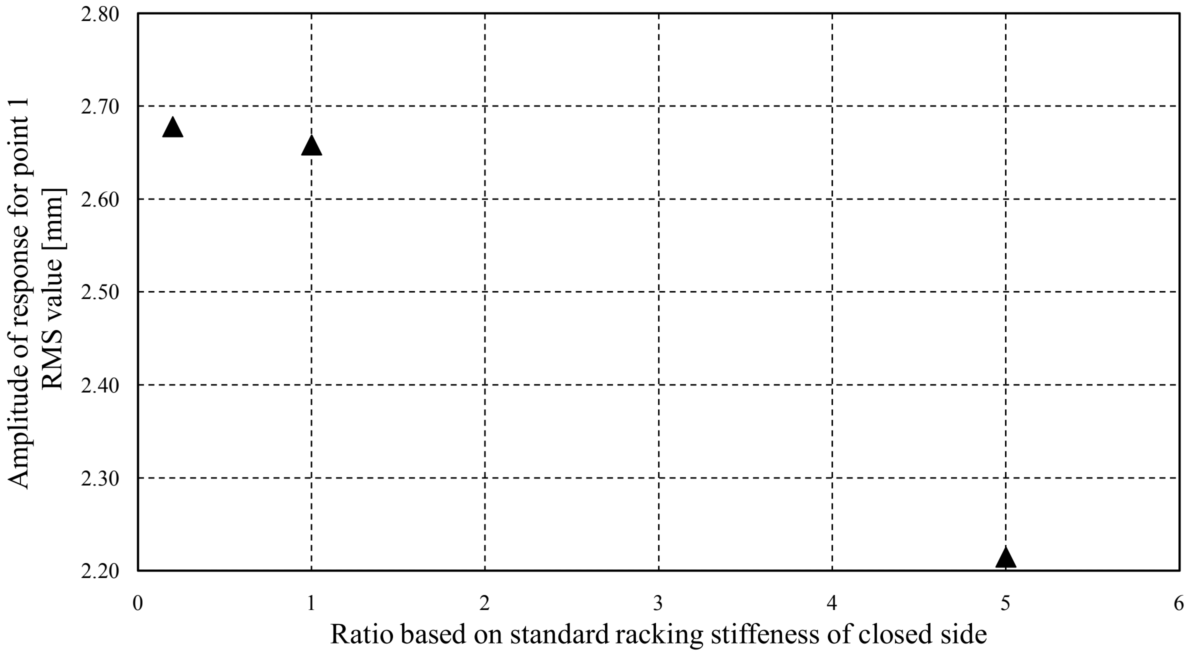

(a) Lateral direction.

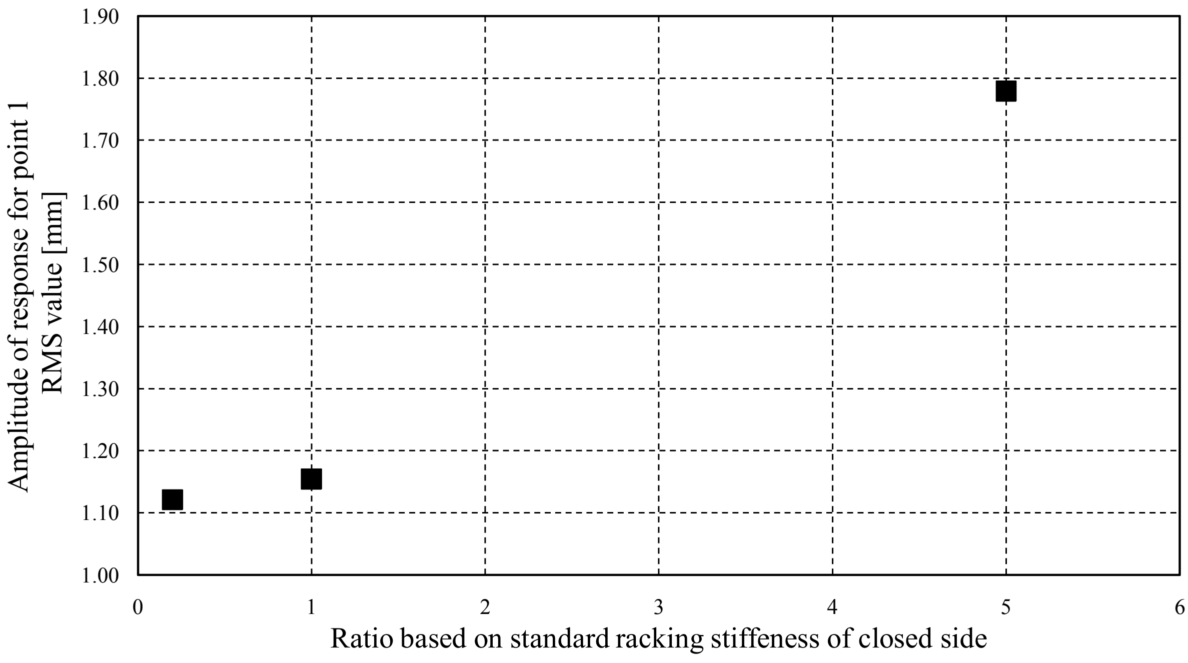

(b) Vertical direction.

Figure 8.6: Effect of changes in racking stiffness on the relative motion of point 1 (RMS value comparison). Case: 7x1–6 mm–2 Hz–1 mm gap–10 degrees–non loaded.

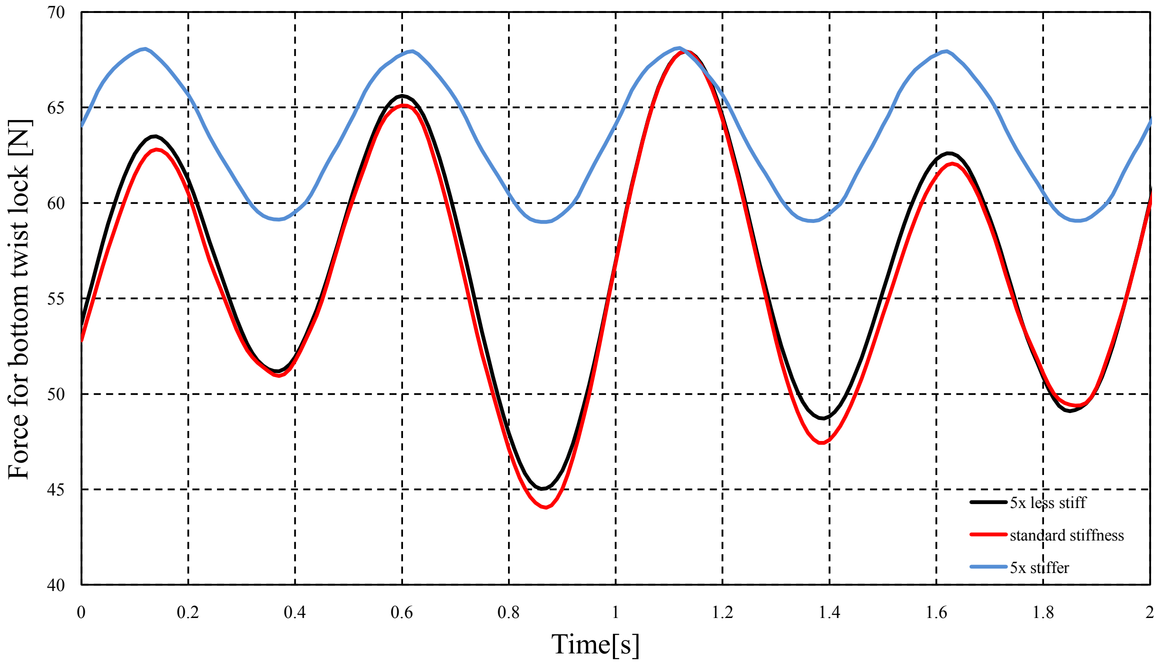

(a) Lateral component.

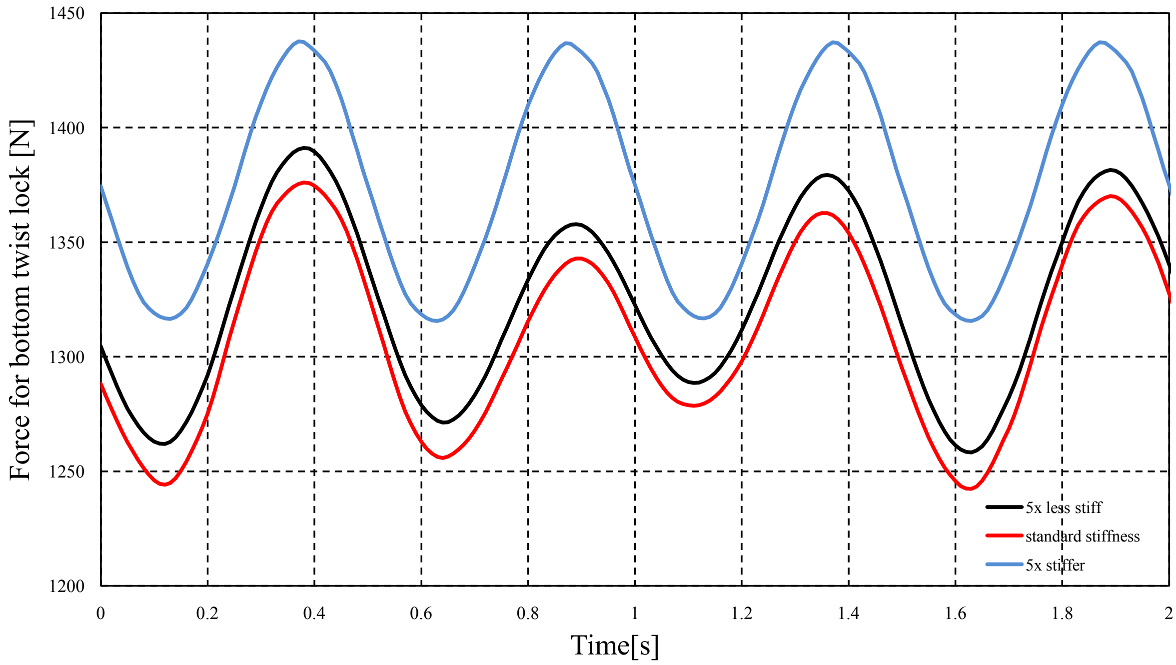

(b) and vertical component.

Figure 8.7: Effect of changes in racking stiffness on twist lock's force. Case: 7x1–6mm–2 Hz–1 mm gap–10 degrees–non loaded.

8.2 Predictions and Advice (7x3)

8.2.1 Pitching

Numerical analysis of the 7x3 system subject to a pitching motion was performed using a model described in the section 7.2.1 and graphically represented in Figure 7.11. As boundary conditions a sinusoidal angular velocity was applied to the base of this system with frequency and amplitude following conditions described in table 8.1. This angular velocity is restrained to the plane x-z. As input variables, two natural parameters were chosen: angular frequency or pitching frequency and gap size.

Table 8.1: Driving excitation conditions for the pitching cases

Amplitude [degrees]	4		
Frequency [Hz]	0.2	0.1	0.08
Gap [mm]	0	1	2

8.2.1.1 Pitching Frequency

Pitching of a vessel generate upward and downward acceleration forces directed tangentially to the direction of rotation. Physically these forces are dependent on the distance from the pitching axis and the period of the rotation. In fact, this force is directly proportional to the pitching axis distance. Additionally, these forces are inversely proportional to the square of the pitching period. Thus for the effect of changes in the pitching period a similar physical behavior is expected for the forces on the bottom twist lock. This trend can be observed in Figure 8.8.

8.2.1.2 Gap Effect on Pitching

Gap is the responsible for the biggest non-linearities observed in the model. Its effects, in the cases studied, was more influential on the dynamical response than the contact forces among stacks. Observing Figure 8.9a is easy to notice that gap size is a dominant factor in the force experienced by the bottom twist lock. The bigger this size, the higher the values of force are observed on it. This is an interesting finding, with easy physical applications aiming to decrease the values of the peaks observed: just a matter of geometrically changing this gap size in the real twist lock. To have a quantitative idea about the effect of this variable, a decrease of around 1.3% was observed by just decreasing gap size.

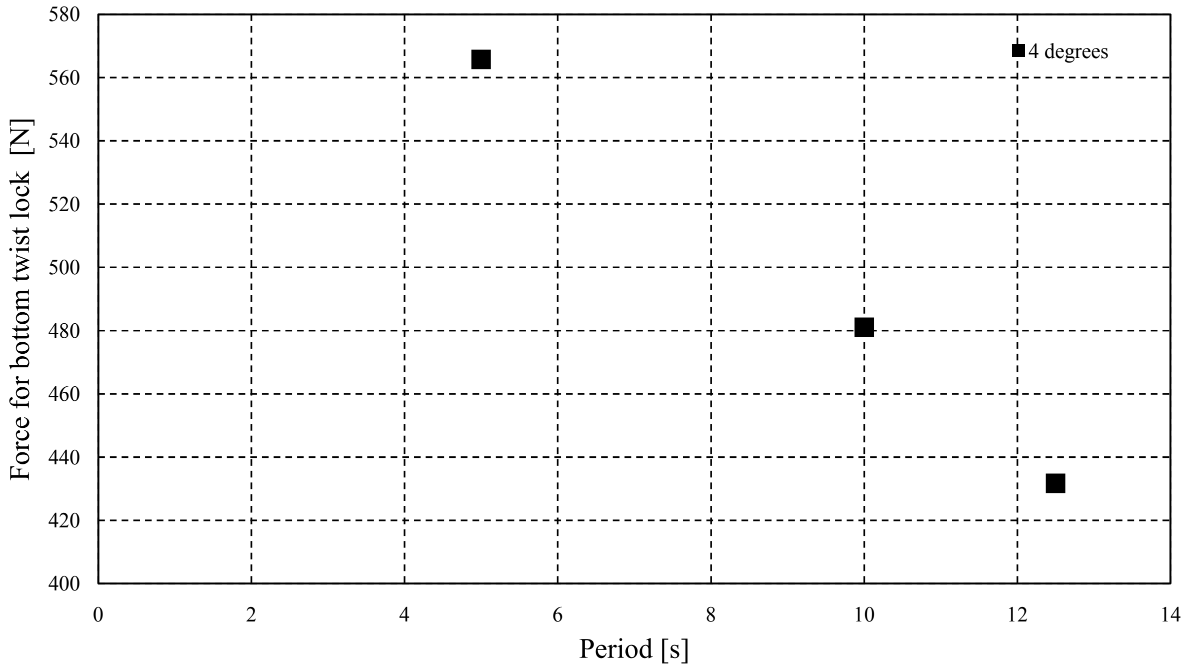

Figure 8.8: Effect of changes in pitching period on twist lock's force (RMS value). Case: 7x3–4 degrees.

8.2.1.3 Damper Effect on Pitching

Second, even not so pronounced like the gap effect, an inclusion of a damper provides a reduction in the maximum values of the force experienced by the bottom twist lock. Again that is a finding with direct practical application and is completely feasible. The effect of a damper is depicted in Figure 8.9b. In terms of reduction, a decrease of around 5% was observed by the inclusion of a damper element.

8.2.2 Rolling

A numerical analysis of the 7x3 system subject to a rolling motion was performed using a model described in the section 7.2.1 and graphically represented in Figure 7.11. As boundary conditions a sinusoidal angular velocity was applied to the base of this system with frequency and amplitude following conditions described in table 8.2. This angular velocity is restrained to the plane y-z. As input variables, three natural parameters were chosen: maximum amplitude angle or maximum rolling amplitude, angular frequency or rolling frequency and gap size.

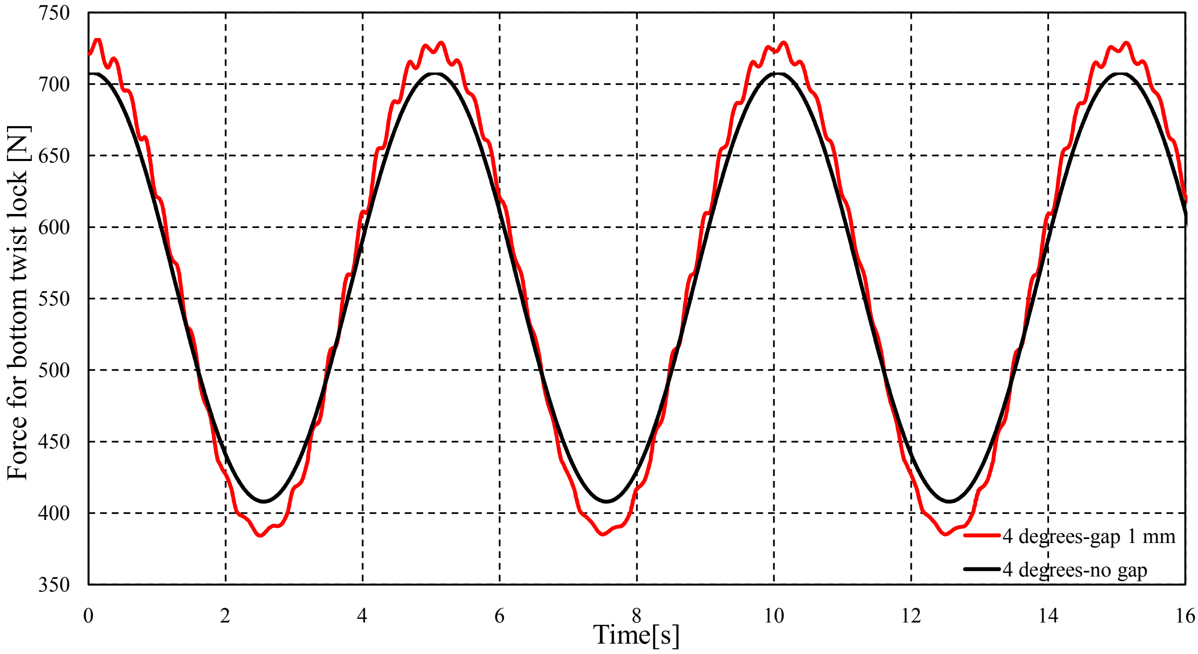

(a) Effect of changes in gap size on pitching.

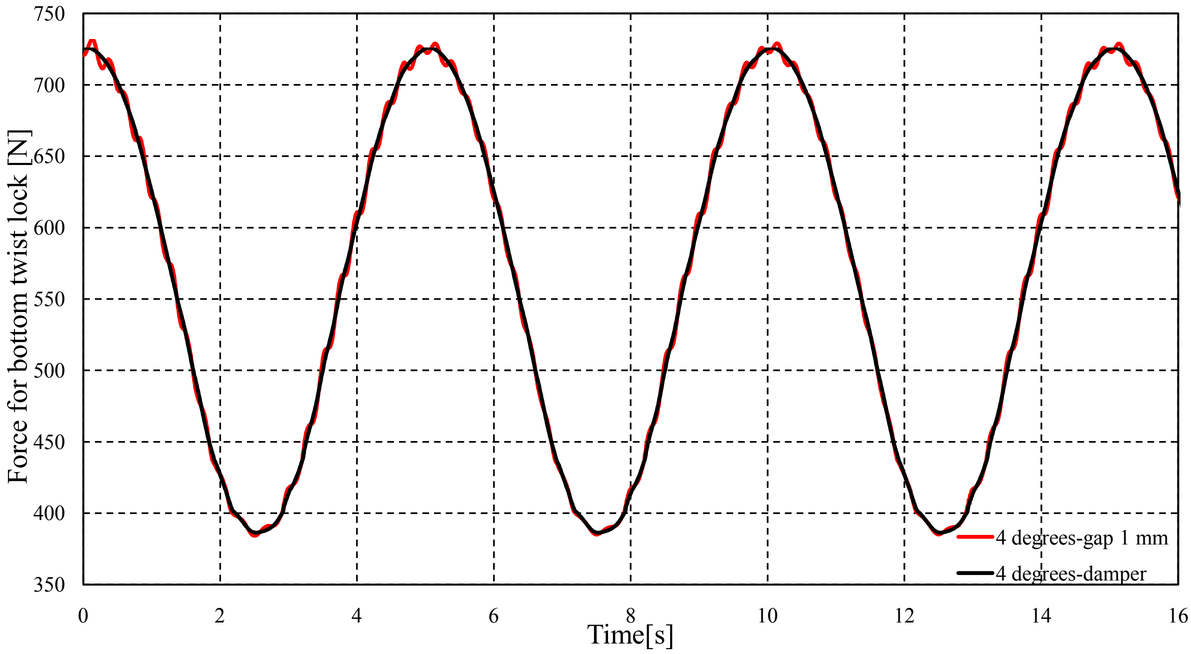

(b) Effectiveness of dampers on pitching.

Figure 8.9: Effect of gap size and damper inclusion (pitching). Case: 7x3–0.2 Hz–4 degrees.

Table 8.2: Driving excitation conditions for the rolling cases

Amplitude [degrees]	10	15	20	25	35
Frequency [Hz]	0.5	0.25	0.05	0.04	
Gap [mm]	0	1	2		

8.2.2.1 Rolling Amplitude

Naturally, amplitude affects the system in a manner proportional to its magnitude, i.e., an increase in the amplitude of the driving excitation induces a direct proportional increase in the force experienced by the bottom twist lock. For example the 0.05 Hz case: the corresponding values for the twist lock's force peak were 1220.53, 1579.30, 2247.68 and 10404.00 N , for the rolling amplitudes of 10, 15, 20 and 35 degrees, respectively. All cases simulated presented consistency in this trend, i.e., presented an response proportional to the rolling amplitude. The overall behavior can be inferred from table 8.3. Furthermore, the trend can be visualized in Figures 8.10a and 8.10b using a time history plot, or Figures 8.11a and 8.11b through a peak value plot.

Table 8.3: Values of force obtained from rolling simulation

	Rolling frequency [Hz]			
	0.04	0.05	0.25	0.5
Rolling amplitude [degrees]	Force [N]			
10	777.06	1220.53	1730.21	2204.60
15	1384.93	1579.30	2348.60	3435.28
20	9996.61	2247.68	2859.34	6184.34
35	10316.00	10404.00	10411.45	10423.90

8.2.2.2 Rolling Frequency

Following the physical behavior of pitching, rolling of a vessel generate upward and downward acceleration forces directed tangentially to the direction of rotation. Physically these forces are dependent on the distance from the rolling axis and the period of the rotation. In fact, this force is directly proportional to the rolling axis distance. Additionally, these forces are inversely proportional to the square of the rolling period. Thus for the effect of changes in frequency a similar physical behavior is expected for the forces on the bottom twist lock. This trend can be observed in Figure 8.12.

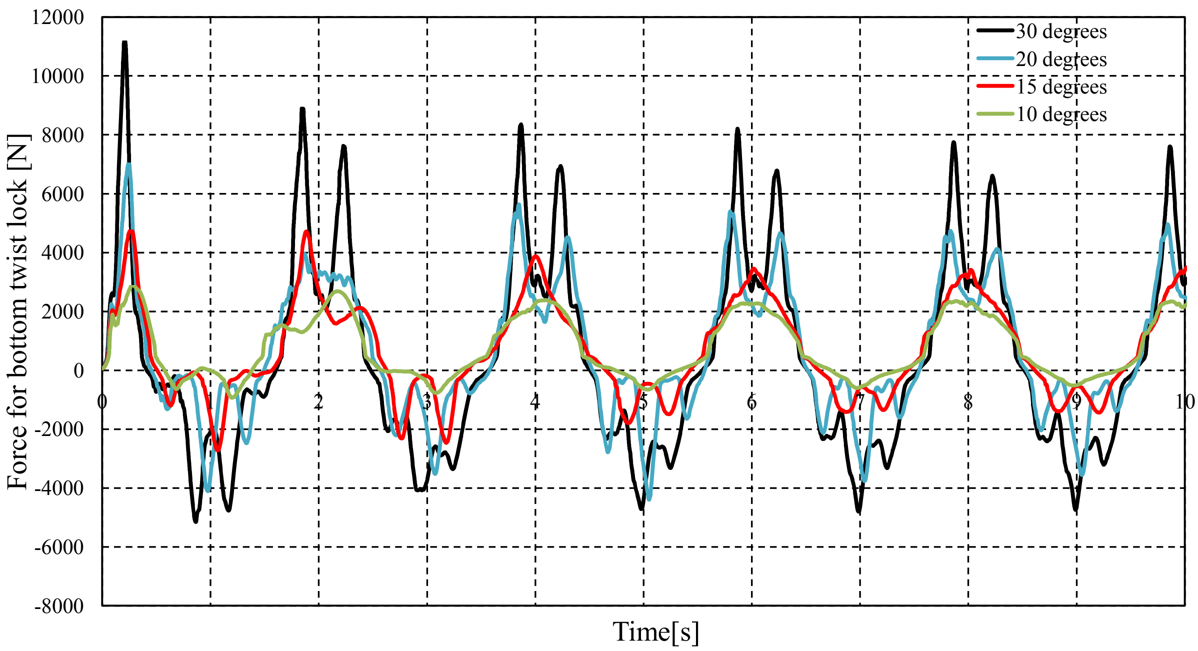

(a) Rolling period of 2 s.

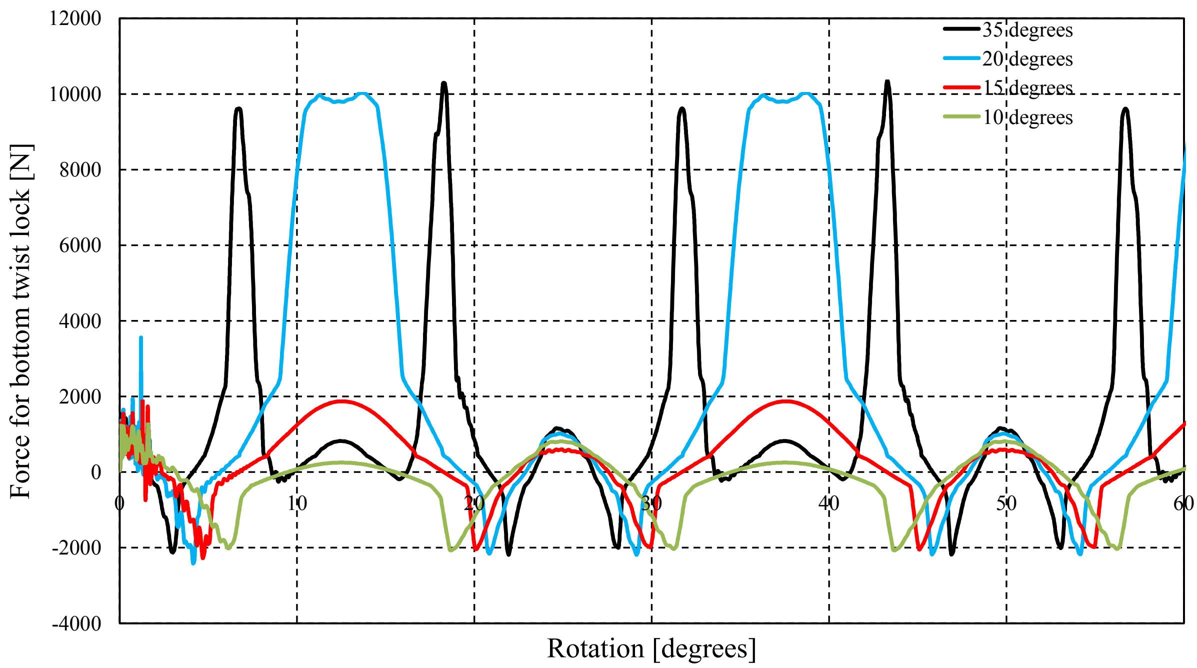

(b) and rolling period of 25 s.

Figure 8.10: Rolling amplitude effect on twist lock's force (Time history comparison).

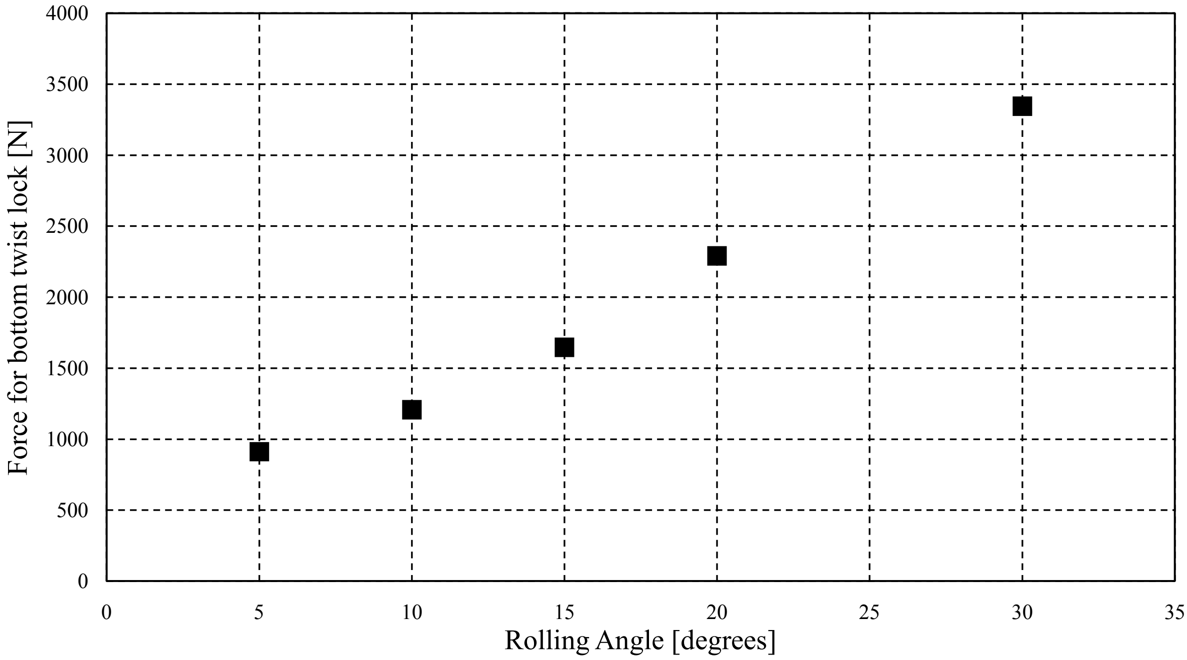

(a) Rolling period of 2 s.

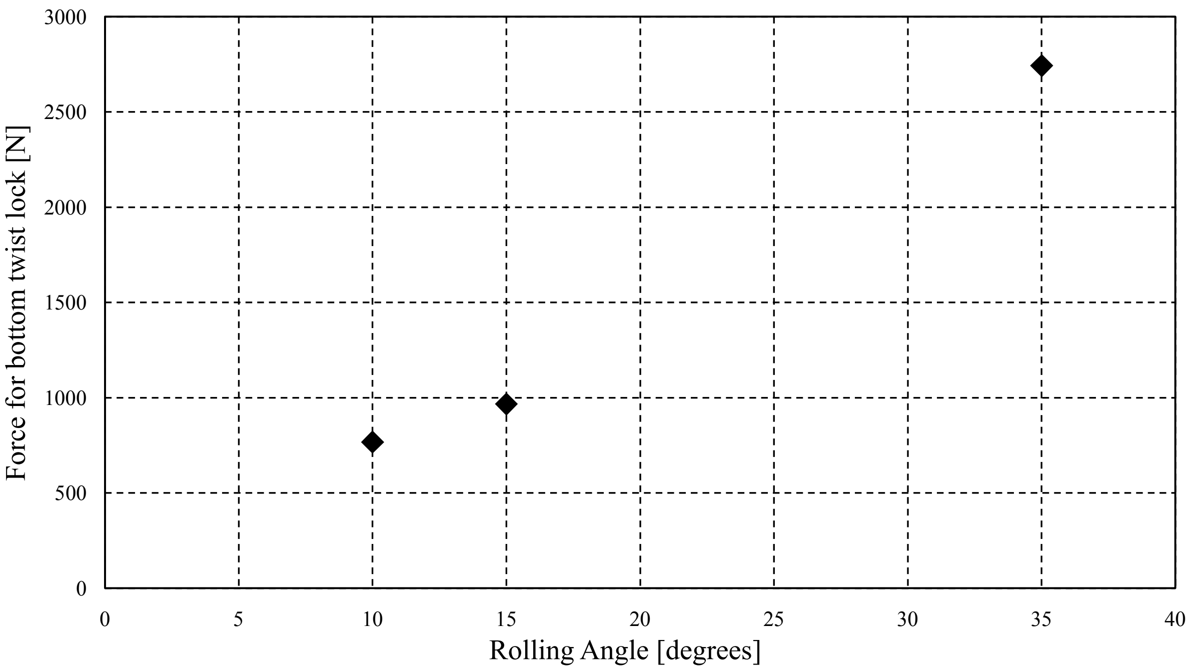

(b) and rolling period of 25 s.

Figure 8.11: Rolling amplitude effect on twist lock's force (Peak value comparison).

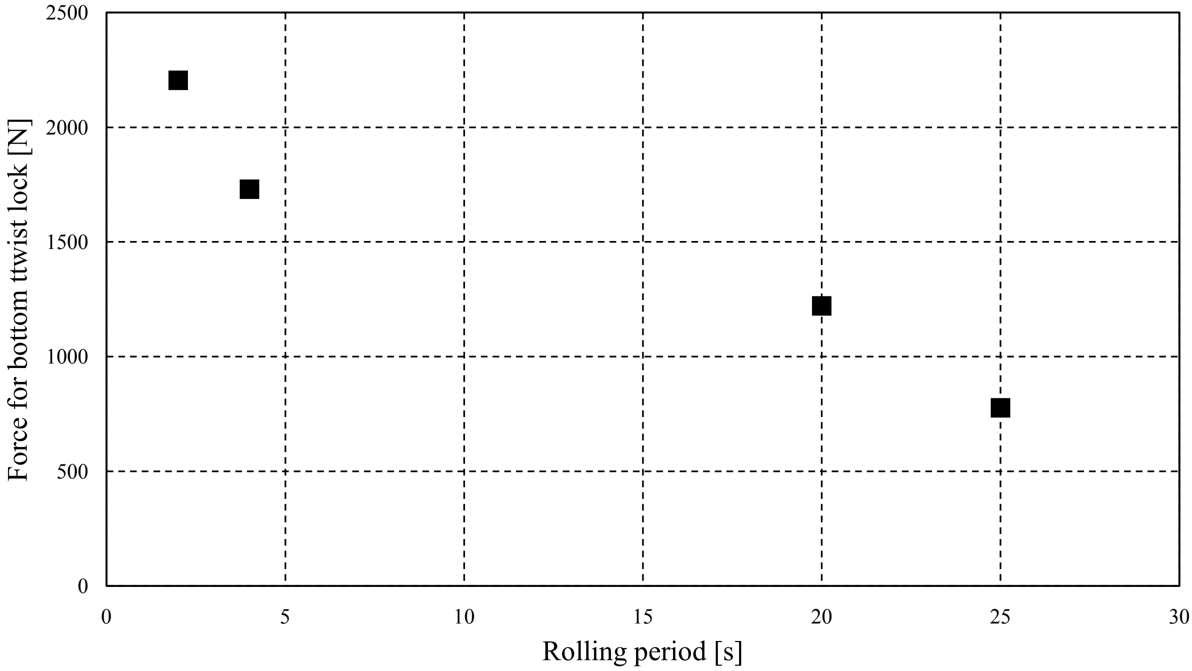

(a) Rolling amplitude of 10 degrees.

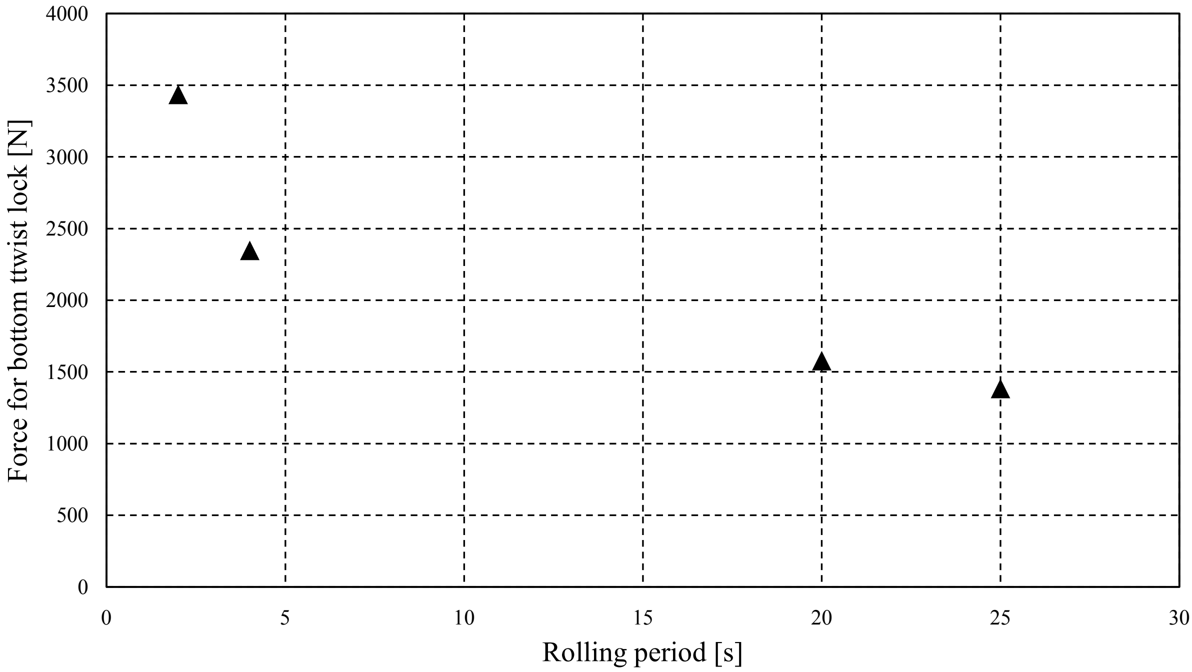

(b) and rolling amplitude of 15 degrees.

Figure 8.12: Effect of changes in rolling period on twist lock's force (RMS value).

8.2.2.3 Gap Effect on Rolling

Following what was observed for pitching, gap is the responsible for the biggest non-linearities observed in the model for rolling, showing similar trends. Its effects, in the cases studied, was more influential on the dynamic response than the contact forces among stacks. Observing Figures 8.13 is easy to notice that gap size is a dominant factor in the force experienced by the bottom twist lock. Like pitching, the bigger this size, the higher the values of force are observed on the twist lock. To have a quantitative idea about the effect of this variable, using RMS values comparison, a decrease of around 54% for the first (Figure 8.13a), and 25% for the second case (Figure 8.13b) were observed by just decreasing gap size by half. It is interesting to emphasize that changes in gap size have effect in all excitations tested for the range of this study.

8.2.2.4 Damper Effect on Rolling

Following what was observed for the gap effect, an inclusion of a damper provides a reduction in the maximum values of the force experienced by the bottom twist lock. Again this is a finding with direct practical application for the industry. However, author is not sure about its feasibility. The effect of a damper is depicted in the Figure 8.15. In terms of reduction, a decrease of around 43% for the first (Figure 8.14a), and 16% for the second case (Figure 8.14b) were observed by the inclusion of a damper element. Important to mention that the value of the damping coefficient (c) played an important role in the force attenuation. For small values of c the attenuation was insignificant. The effect observed in these figures was obtained considering a considerable high value (c=1000 kg/s).

8.2.2.5 Joining Adjacent Corner Castings Effect on Rolling

Another alternative to decrease the energy transferred among stacks because of the impact among them is to remove the pounding through decreasing lateral motion. An efficient way to decrease that lateral motion, and consequently minimize the impact, is to join the adjacent structures in critical locations so their motion can be in phase with one another. This technique is not new, many researchers pointed out the advantages of this approach: Kasai *et al.* [40], Abdullah *et al.* [1], Jankowski *et al.* [39], Ruangrassamee & Kawashima [66], Kawashima & Shoji [41], Raheem [61] and Sharma [70]. However, up to now this technique has being applied in seismology to mitigate the noxious effects of earthquakes. For the rolling cases studied the decrease observed for the first case was 31% (Figure 8.15a), and 37% for the second case (Figure 8.15b).

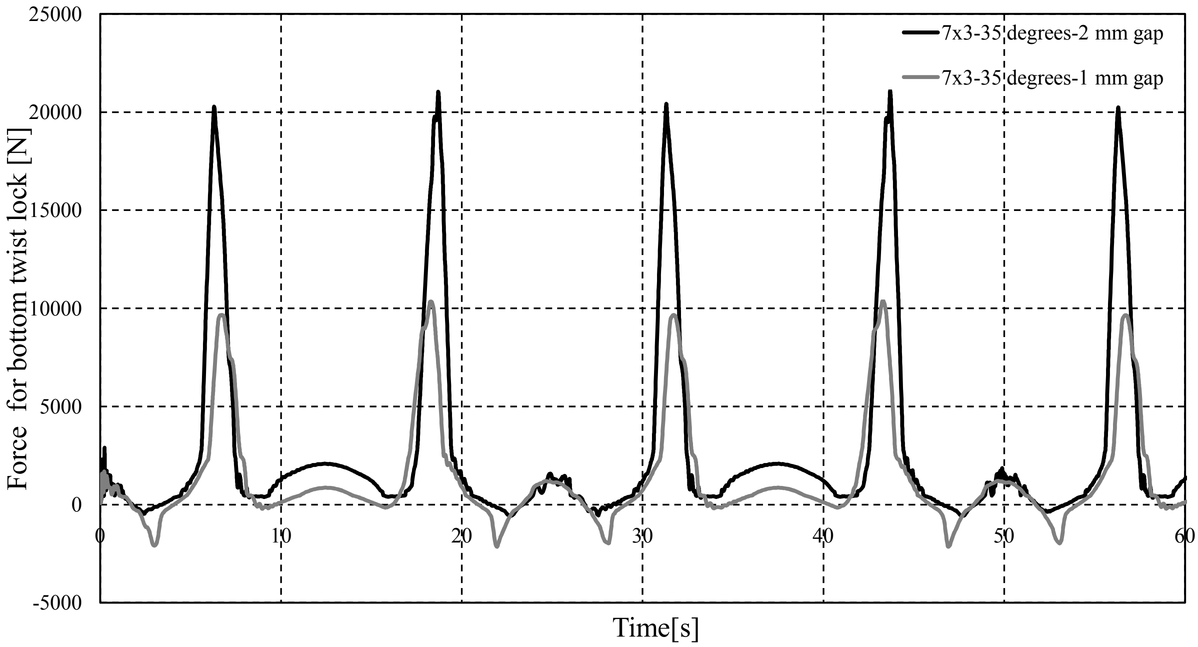

(a) Case: 35 degrees and 0.04 Hz.

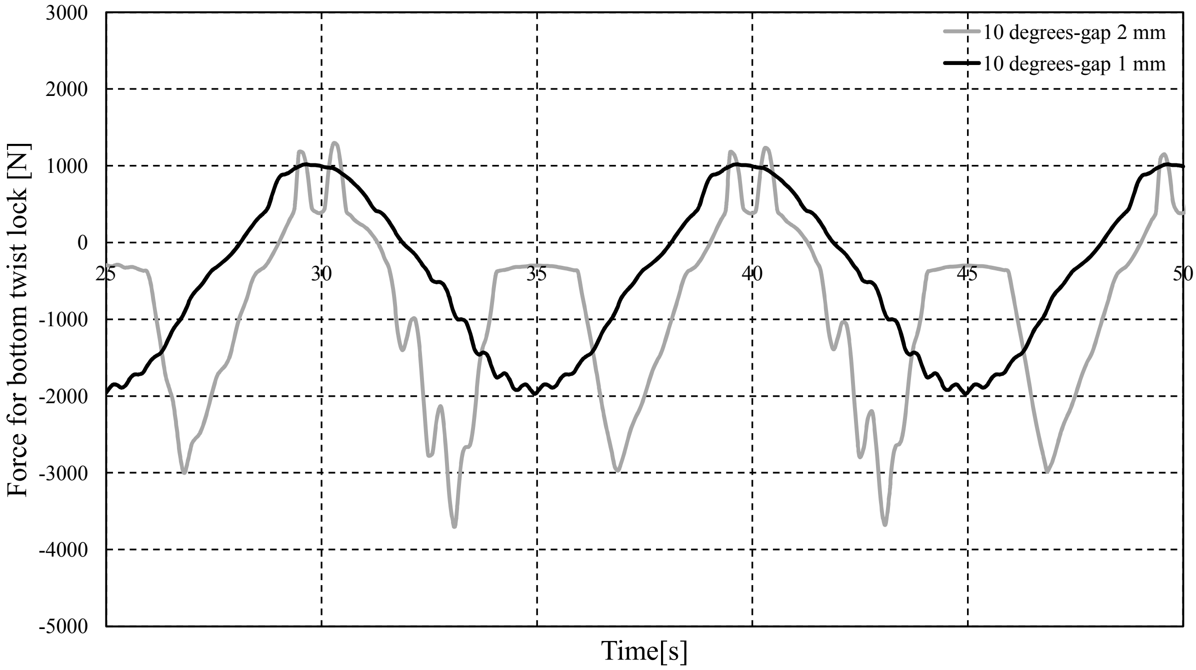

(b) Case:10 degrees and 0.1 Hz.

Figure 8.13: Effect of changes in gap size (rolling).

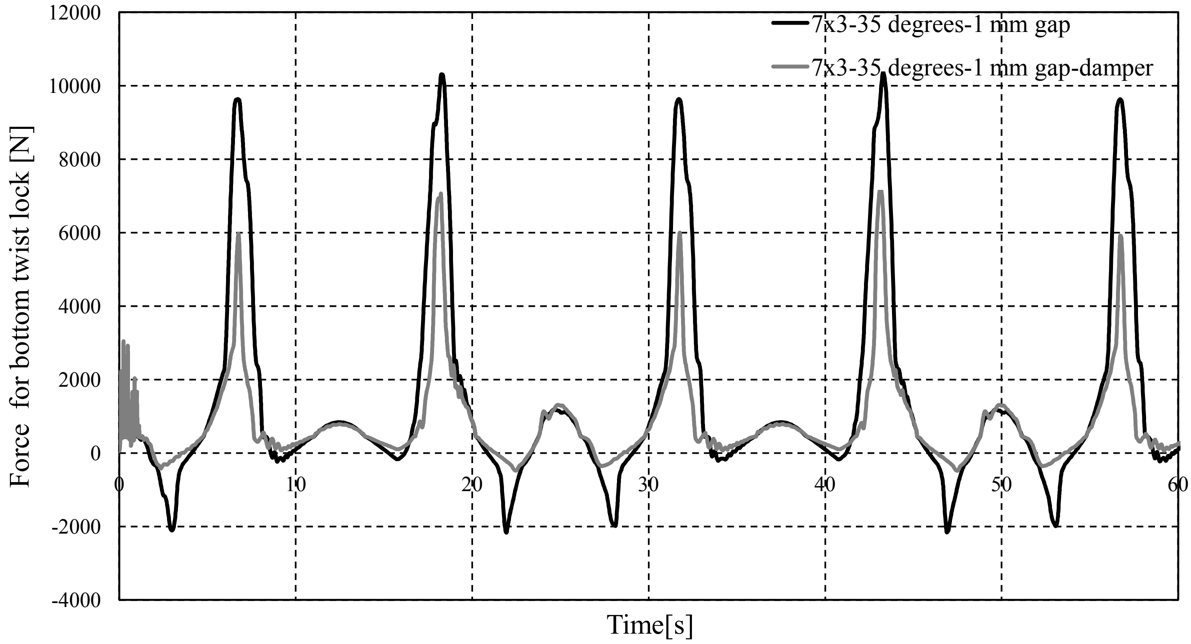

(a) Case: 35 degrees and 0.04 Hz.

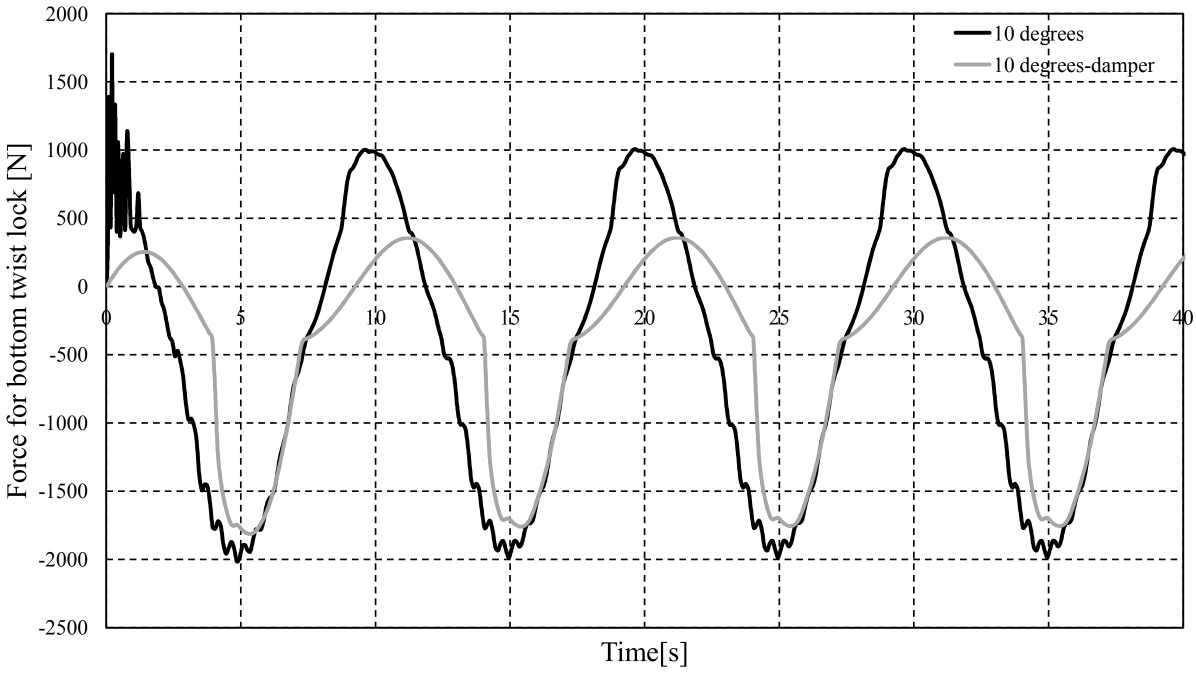

(b) Case:10 degrees and 0.1 Hz.

Figure 8.14: Effectiveness of dampers (rolling).

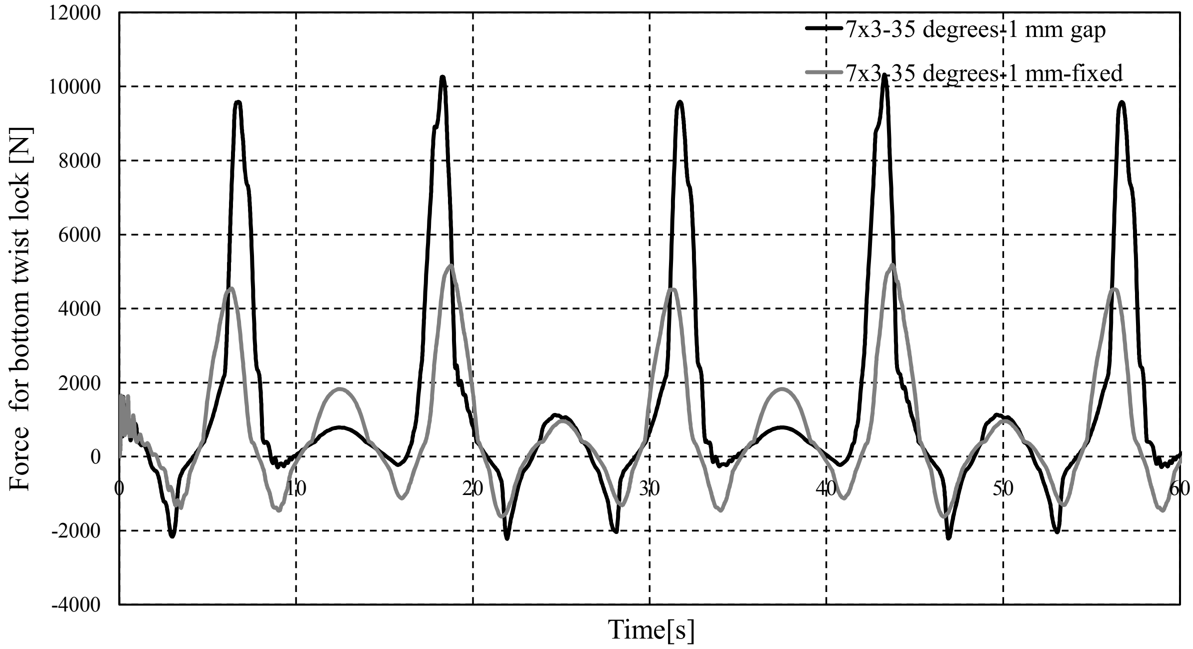

(a) Case: 35 degrees and 0.04 Hz.

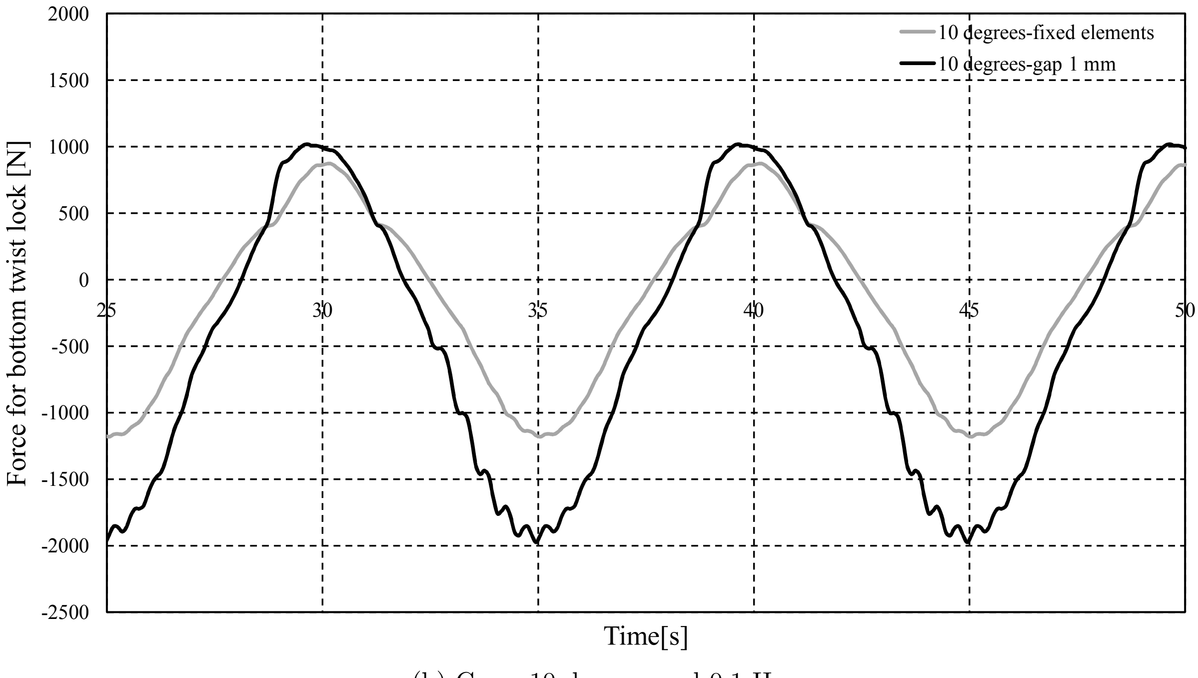

(b) Case: 10 degrees and 0.1 Hz.

Figure 8.15: Effectiveness of joining adjacent stacks (rolling).

8.3 Limitations of the Study

However, some limitations most be pointed out to qualify and fully understand the overall results obtained from our approach. Some disadvantages involved:

- For the scaling stage of this study, the choice of specific parameters may lead to a loss of a complete similarity, an idealized situation, that all scaling laws are satisfied simultaneously. If this is the case, some authors refer to it as *partial similarity*, i.e, a system where at least one of the similarity conditions cannot be satisfied [64]. The consequences are a clear by-product of it: behavior amidst both systems may be significantly different.

- Real containers during marine transportation are under the influences of many physical parameters that are sometimes difficult to emulate during experimentation, i.e., their number is so imposing imposing that is impractical to include all of them in an experiment. Thus, the best choice is to selectively elect parameters that represent dominant physical effects like the ones used for the experiments. However, some important parameters were excluded in some stages , e.g., amplitude and frequency (secondary importance) of driving excitation, payload and gap size for the 7x3 cases. These exclusion limited greatly the qualification of the numerical model.

- 7x3 experimental study has only three cases, which obligates the author to be extremely cautious about the results from this system. In other words, correlation of many variables could not be obtained experimentally, limiting the calibration of the numerical model. Consequently, limiting the predictions that can be drawn from this model.

- A crucial variable was omitted during the study of the 7x3 case: gap size. Together with contact between adjacent stacks this variable is the source of the non-linearities observed in the studies. Thus, should have been included in a larger variety of experimental cases.

- Another variable that might contribute for the understanding of the dynamic behavior of the container stacks is the payload. From the 7x1 cases data analysis it is clear the payload influence on the response. However, it would be more interesting and more realistic to perform experiments using this variable in the 7x3 configuration.

- In general, results and predictions from the numerical model are reasonable. However, for the low values of frequency disparities between experimental and numerical data were too common. In this view, authors must be cautious and state that the numerical model is valid for a bounded frequency range.

- Numerical model did not include contact, and consequently friction, for the corner castings in the same stack. This exclusion may help the appearance of discrepancies specially in cases where the container stack is tilted or under motions like pitching and rolling.

- Ship's motion simulated in this study considered an axis located in the inferior portion of the rigid base. However for real ships this center of rotation is located in the center of gravity. Main movements in the ship, like pitching and rolling, have a strong influence from the distance from the rotation axis. Thus adjustment of this distance is an important step to understand the container stack dynamics completely.

- Movements were considered separately and not a combination like the ones encountered during maritime transportation. Because of the non-linearities presented in the model one cannot assume that the linear superposition principle is valid for this system and analyze each movement separately.

- The effectiveness of passive control like dampers is still difficult to prove and strongly dependent on frequency, which brings the necessity of more studies.

Chapter 9

Conclusions

9.1 Summary of Findings

This project was undertaken to investigate the fundamental mechanical behavior of a container stack under controlled vibrational parameters and to provide advice from the numerical-analysis based predictions. The study helped to elucidate some points regarding the system's fundamental mechanical behavior, where correlation of dynamic properties depending on amplitude, frequency, base rotation, container load and twist lock gap size, were obtained and used to calibrate and validate a numerical model. After this strenuous validation, the scaled numerical model was used as a valid tool to simulate the behavior of multi-stack configuration in some simple situations faced by containers during maritime transportation. Among these situations some common forces exerted on the containers were studied in detail: heaving, pitching and rolling, employing cases reported in the literature. Additionally, the problem of how simple changes in basic variables affect force in the bottom twist lock was addressed providing useful advice for the industry, trying to maintain the problem complexity to a minimum. Undoubtedly, this is one of the most significant findings to emerge from this study. In this panorama, it may contribute significantly to the understanding of container stack dynamics, an area where intuition and old standards are still preferred over more solid scientific principles.

It is well-known that the loss of containers on ocean-going ships can be reduced by the following measures: practicable methods for determining the weight of containers accurately, stowing cargo securely and safely in containers, lashing deck containers securely on board the ship, making more use of weather information and route advisory services, adjusting the course and speed of the ship to its loading condition and the weather situation, a wave radar that notifies the ship's command of high waves at a long distance and even at night and a system which in combination with a wave radar provides timely warning of the danger of parametric rolling could likewise help to reduce losses. However, the findings of this study suggest some extra courses of action to prevent container losses:

- Changing twist lock geometry, through a simple decrease in gap size is a good and viable solution to decrease response,
- Inclusion of viscous damping elements in the twist lock geometry is another measure however this measure has a significant effect only when the driving excitation frequency is within a margin of 20% around the natural frequency of the system,
- Changes in stiffness (increase) produce a significant effect in the response but are not practicable and,
- Placing the heaviest container on the first tier is another factor that must be taken into account.

9.2 Answer to the Central Question of this Dissertation

Returning to the first question posed at the beginning of this investigation, whether or not the dynamic effect or impact among stacks is an important phenomenon in container stack dynamics, it is now possible to state, supported by enough body of evidence from experimental and numerical data, that this phenomenon is non-negligible. The same can be stated about the second question, whether or not the impact among stacks have an important role in the dynamics of the system, it is non-negligible phenomenon. Experimental and numerical evidence support my claim. The overall behavior of the container stack dynamics can be classified as non-linear because of two sources: twist lock gap and the impact among stacks. Therefore, the study has gone some way towards enhancing our understanding of the container stacks dynamics.

To understand their weights in the overall behavior two extra simulations were idealized. The main goal was to evaluate quantitatively their effects. Both simulation considered a single stack with distinct twist lock configurations: the first one neglects the gap, and the second one includes the gap. The results, as shown in Figure 9.1, indicate that gap size and impact are the main sources of the non-linearities observed for the system. Furthermore, there is a significant positive correlation between both variables and the force experienced by the bottom twist lock. The inclusion of a gap in the system increased the force on the bottom twist lock by 69%. The other case simulated showed that the impact among stacks represented an increase of 96% on that force.

The simulation cases tried to emulate an extreme case of parametric rolling reported by France and colleagues [27] that victimized a container ship 1998. The conditions resulted in a loss of 400 containers at sea. However, with a small number of cases studied, caution must be applied, as the findings might not be transferable to all conditions faced by the container stacks. In other words, it is possible to hypothesize that, for small rolling amplitudes, these significant increases are less likely to occur. Although, one of the issues that emerges from these findings is that the current standards to calculate the fixings elements in the container stacks may not be appropriate keeping in mind that the calculation of the current standards do not consider dynamical forces explicitly.

9.3 Future Work

- Analyze the response of other points, e.g. , points 2 and 3 in the 7x1 case and points 2, 3, 6, 7, 8, and 9 in the 7x3 case. This kind of analysis can give important information about how the stack tilts under the conditions used for the study. Additionally, it can be an important step to validate the numerical model to simulate racking of the stack.
- Important parameters were excluded in some stages , e.g., amplitude and frequency of driving excitation, payload and gap size for the 7x3 cases. Such parameters are an area where further studies are needed.
- Combinations of motions should be used as driving excitation for the numerical cases and not motions individually.
- The use of base isolation systems seems to be an interesting approach to minimize the problem of container loss.

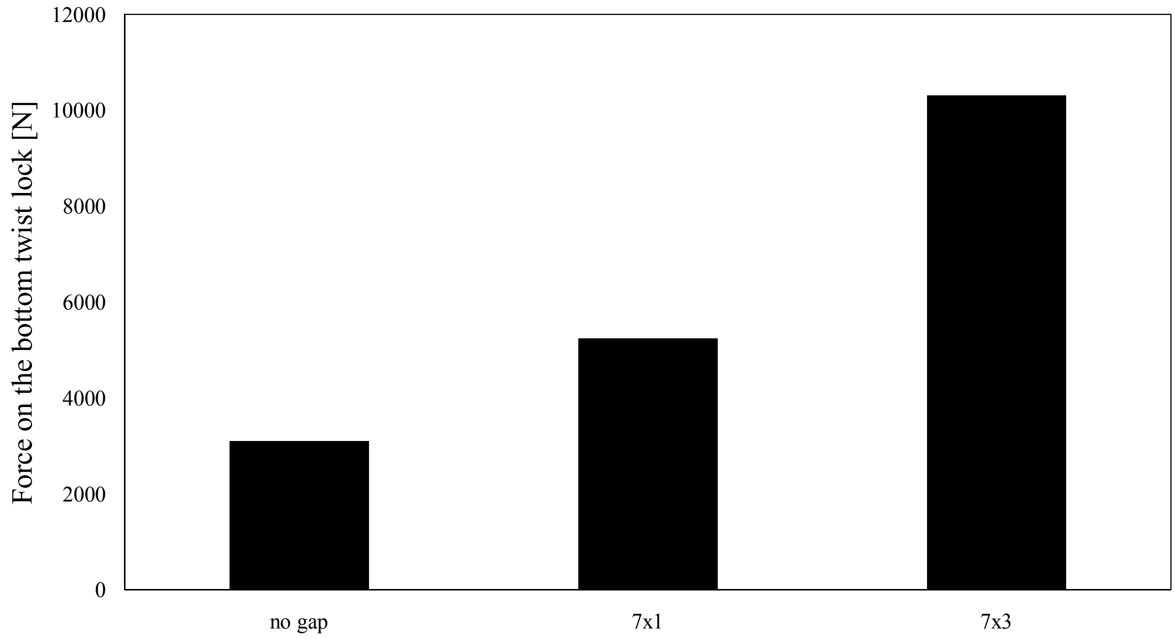

(a) RMS value comparison.

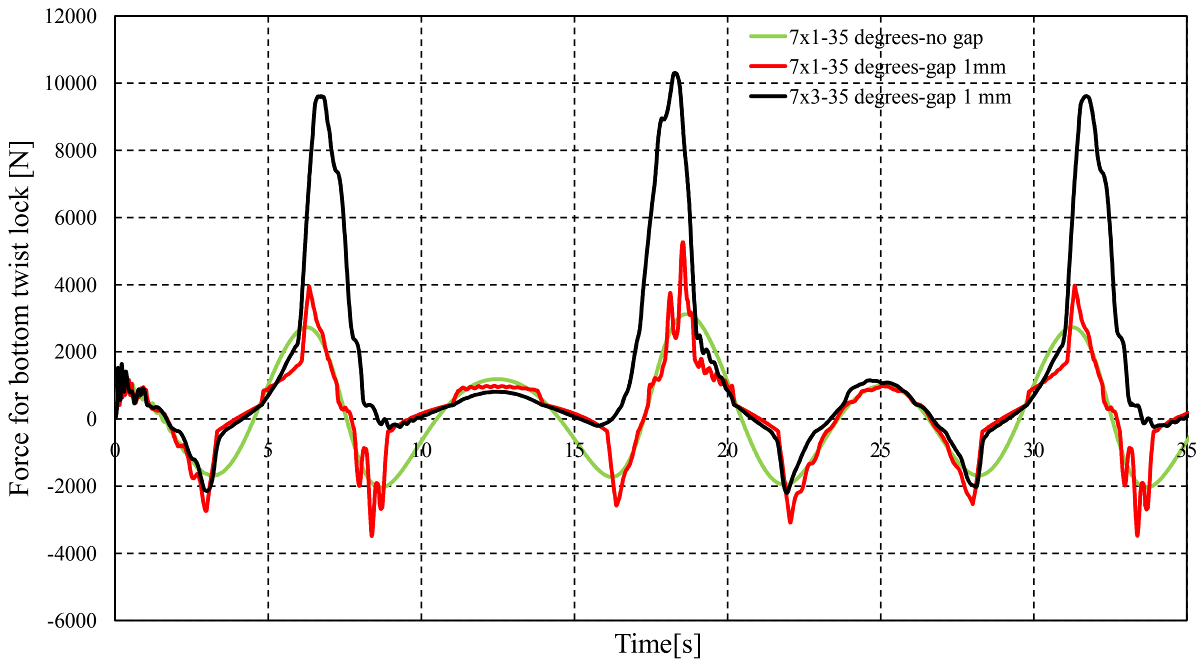

(b) Time history comparison.

Figure 9.1: Quantification and identification of the sources of the system non-linearities.

Appendix A

Full scale model

An initial simplified full scale model was build based on the information provided by the International Organization For Standardization (ISO). Dimensions and ratings were obtained from ISO668 [35] and structural stiffness information from ISO1496 [36]. The parameters chosen to build the full scale model are identical to the ones were used to build the scaled model from the Froude scaling laws. Namely:

- Dimensions: length, width and height
- Mass
- Moments of inertia
- Transversal racking stiffness of front (open) end frames
- Transversal racking stiffness of rear (closed) end frames
- Longitudinal racking stiffness
- Torsional stiffness

The full scale model presented good results for linear and non-linear cases as can be seen in Figures A.1 and A.2. The ratio of the RMS values for the cases presented in these figures are 64.14 and 64.02 for the linear and non-linear cases, which are close the the theoretical value of 64.

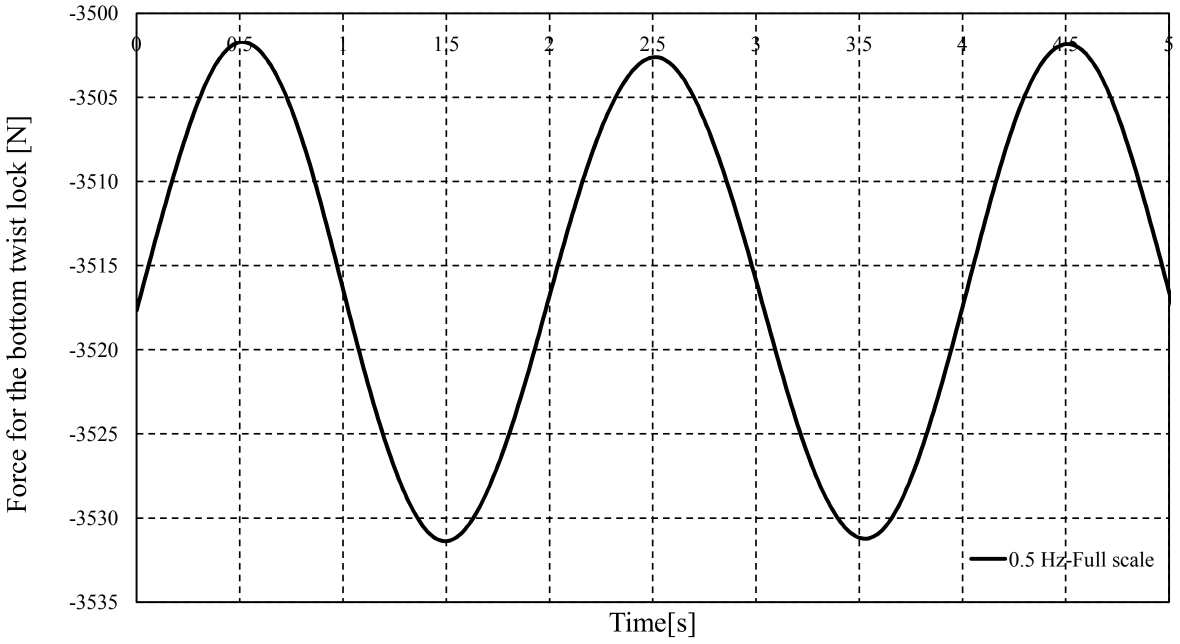

(a) Full scale model.

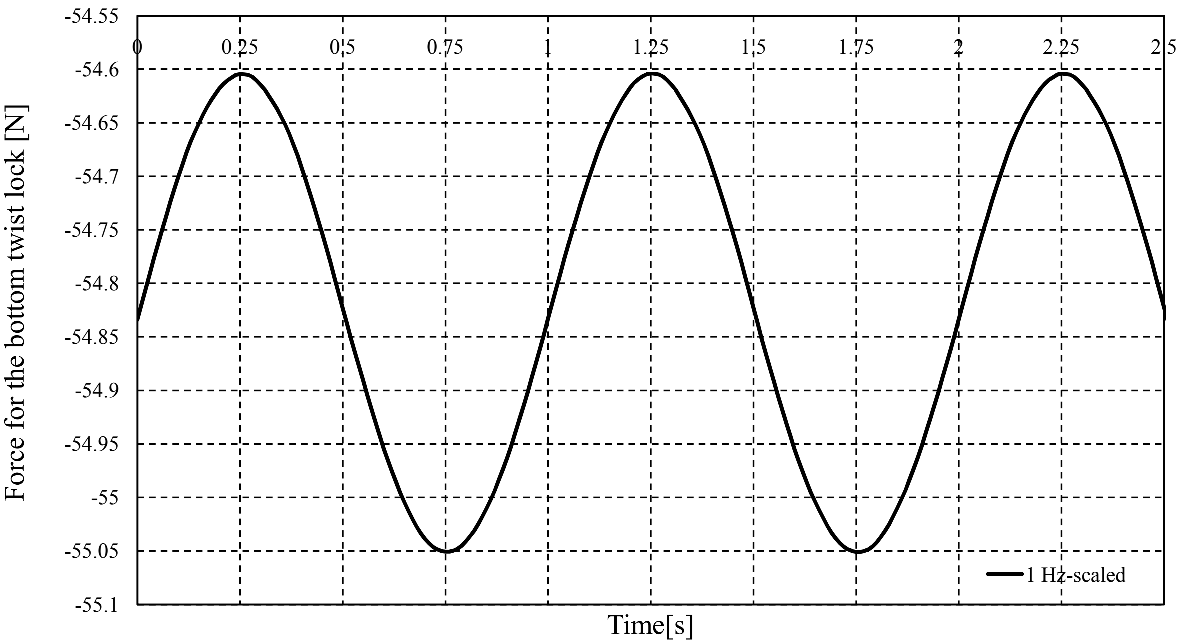

(b) Scaled model.

Figure A.1: Comparison of full and scaled model results (linear case).

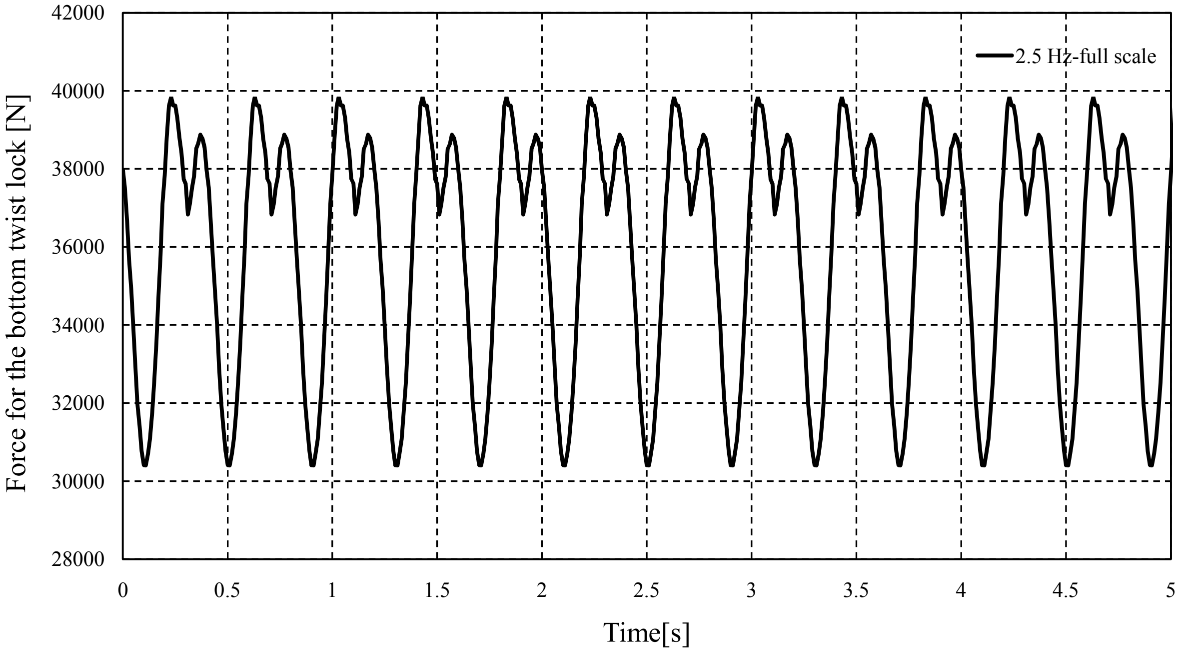

(a) Full scale model.

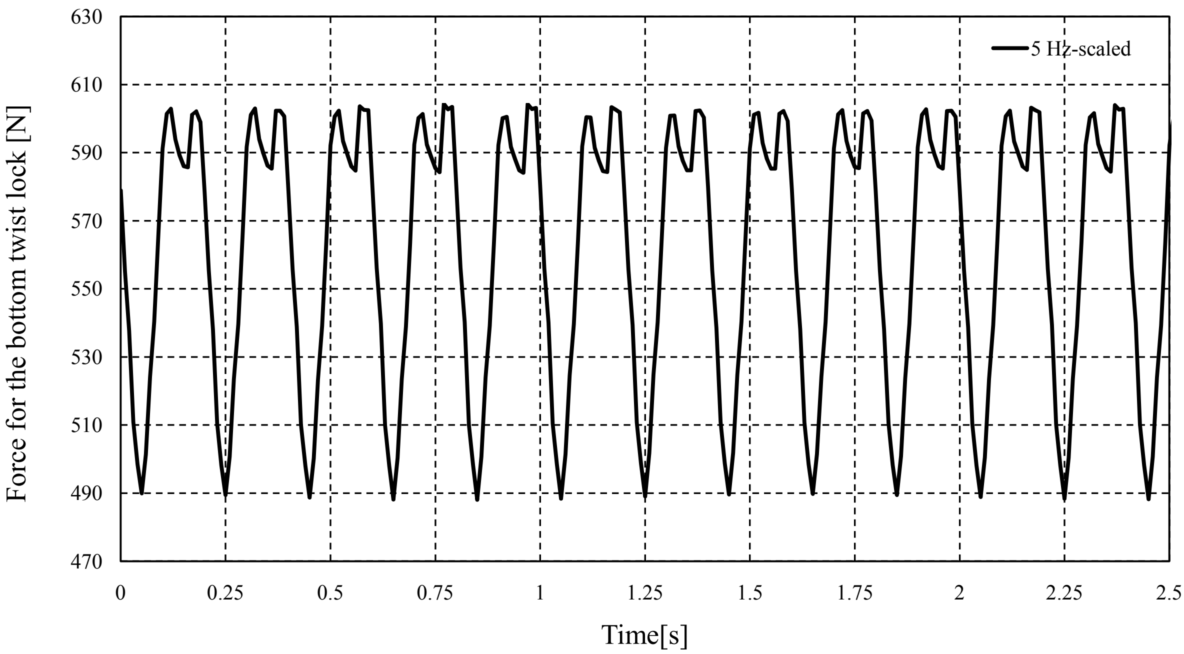

(b) Scaled model.

Figure A.2: Comparison of full and scaled model results (nonlinear case).

Table A.1: Geometric scaling of the similitude parameters for the models considering a 20 ft container based on ISO [36]

		Full-scale(20 ft)	Numerical model
External dimensions	length[m]	6.058	6.058
	width[m]	2.438	2.438
	heigth[m]	2.591	2.591
Mass [kg]		2330	2330
Moment of Inertia	I_{xx}[kg/m^2]	3765	3765
	I_{yy}[kg/m^2]	11830	11830
	I_{zz}[kg/m^2]	11486	11486

References

[1] Abdullah, M., Hanif, J., Richardson, A. & Sobanjo, J. (2001). Use of a shared tuned mass damper (STMD) to reduce vibration and pounding in adjacent structures. *Earthquake Engineering & Structural Dynamics*, **30**, 1185–1201. 155

[2] Adhikari, S. (2006). Damping modelling using generalized proportional damping. *Journal of Sound and Vibration*, **293**, 156–170. 86

[3] Aguiar, V.S., Kirkayak, L., Suzuki, K., Futaoka, Y. & Sueoka, H. (2009). Nonlinear dynamic simulation of container stack. *Conference of the Japan Society of Naval Architects and Ocean Engineers–JASNAOE*. 25

[4] Aguiar, V.S., Kirkayak, L. & Suzuki, K. (2010). Non-linear dynamic simulation of container stack collapse. *Proceedings of the Japan Society for Computational Engineering Conference–JSCES*, **15**. 25

[5] Aguiar, V.S., Kirkayak, L., Suzuki, K., Sueoka, H. & Ando, H. (2010). Development of a method to analyze container stack non-linear dynamics. *Conference of the Japan Society of Naval Architects and Ocean Engineers–JASNAOE*. 26

[6] Anagnostopoulos, S. (1988). Pounding of buildings in series during earthquakes. *Earthquake Engineering & Structural Dynamics*, **16**, 443–456. 92

[7] Anagnostopoulos, S. (2004). Equivalent viscous damping for modeling inelastic impacts in earthquake pounding problems. *Earthquake Engineering & Structural Dynamics*, **33**, 897–902. 92

[8] Anagnostopoulos, S. & Spiliopoulos, K. (1992). An investigation of earthquake induced pounding between adjacent buildings. *Earthquake Engineering & Structural Dynamics*, **21**, 289–302. 92

[9] Bathe, K. & Wilson, E. (1976). *Numerical methods in finite element analysis*. Prentice-Hall Englewood Cliffs, NJ. 84

[10] BENDAT, J. & PIERSOL, A. (2010). *Random data: analysis and measurement procedures*. Wiley. 40

[11] BRIDGMAN, P. (2007). *Dimensional Analysis*. Read Books. 50

[12] BUCKINGHAM, E. (1914). On physically similar systems; illustrations of the use of dimensional analysis. *Physical Review*, **IV**, 345–376. 50

[13] BUCKINGHAM, E. (1915). Model experiments and the forms of empirical equations. *American Society of Mechanical Engineers Transactions*, **37**, 263–292. 50

[14] BUCKLE, I. & MAYES, R. (1990). Seismic isolation: history, application, and performanceA world view= Isolation sismique: histoire, applications, performances. Panorama mondial. *Earthquake spectra*, **6**, 161–201. 138

[15] BURSI, O. & WAGG, D. (2008). Modern Testing Techniques for Structural Systems. 54

[16] CAUGHEY, T. & OKELLY, M. (1964). Classical normal modes in damped linear dynamic systems(Classical normal modes in discrete and continuous viscously damped linear dynamic systems). In *American Society of Mechanical Engineers, Winter Annual Meeting, New York, N. Y; United States*, 6. 84

[17] CHANG, K., LIN, Y. & CHEN, C. (2008). Shaking Table Study on Displacement-Based Design for Seismic Retrofit of Existing Buildings Using Nonlinear Viscous Dampers. *Journal of Structural Engineering*, **134**, 671. 31

[18] CHAU, K., WEI, X., GUO, X. & SHEN, C. (2003). Experimental and theoretical simulations of seismic poundings between two adjacent structures. *Earthquake Engineering and Structural Dynamics*, **32**, 537–554. 94

[19] CHOWDHURY, I. & DASGUPTA, S. (2003). Computation of Rayleigh damping coefficients for large systems. *The Electronic Journal of Geotechnical Engineering*, **8**. 87

[20] CHUNG, W., YUN, C., KIM, N. & SEO, J. (1999). Shaking table and pseudodynamic tests for the evaluation of the seismic performance of base-isolated structures. *Engineering Structures*, **21**, 365–379. 31

[21] COLE, G., DHAKAL, R., CARR, A. & BULL, D. (2010). Building pounding state of the art: Identifying structures vulnerable to pounding damage. *Wellington, NZ*, 26–28. 92

[22] Conoscente, J., Hamburger, R. & Johnson, J. (1992). Dynamic analysis of impacting structural systems. In *Proceedings of the Tenth World Conference on Earthquake Engineering. AA Balkema: Rotterdam*, 3899–3903. 94

[23] Constantinou, M. & Symans, M. (1993). Seismic response of structures with supplemental damping. *The Structural Design of Tall Buildings*, **2**, 77–92. 138

[24] Courant, R., Friedrichs, K. & Lewy, H. (1928). On the partial difference equations of mathematical physics. *Mathematische Annalen*, **100**, 32–74. 94

[25] Cudahy, B. (2006). The containership revolution. *Transportation Research Board of the National Academies*, **246**, 5–9. 2

[26] Ege, K., Boutillon, X. & David, B. (2009). High-resolution modal analysis. *Journal of Sound and Vibration*, **325**, 852–869. 61

[27] France, W., Levadou, M., Treakle, T., Paulling, J., Michel, R. & Moore, C. (2003). An investigation of head-sea parametric rolling and its influence on container lashing systems. *Marine technology and SNAME news*, **40**, 1–19. 12, 144, 163

[28] Fraraccio, G., Brügger, A. & Betti, R. (2008). Identification and Damage Detection in Structures Subjected to Base Excitation. *Experimental Mechanics*, **48**, 521–528. 31

[29] Froude, W. (1874). *On useful displacement as limited by weight of structure and of propulsive power*. Institution of Naval Architects. 50

[30] Gabbay, D., Meijers, A., Thagard, P. & Woods, J. (2009). *Philosophy of Technology and Engineering Sciences*. North-Holland. 49

[31] Goland, M., Wickersham, P. & Dengler, M. (1955). Propagation of elastic impact in beams in bending. *Journal of Applied Mechanics*, **22**, 1–7. 92

[32] Goldsmith, W. (2001). *Impact: the theory and physical behaviour of colliding solids*. Dover Pubns. 92, 94

[33] Hanson, R. (1993). Supplemental damping for improved seismic performance. *Earthquake spectra*, **9**, 319–334. 138

[34] Harris, H. & Sabnis, G. (1999). *Structural modeling and experimental techniques*. CRC. 31

[35] ISO (1990). *Series 1 freight containers–Specification and testing–Part 1: General cargo containers for general purposes*. International Organization For Standardization. 55, 165

[36] ISO (1995). *Series 1 freight containers – Classification, dimensions and ratings*. International Organization For Standardization. 9, 57, 165, 168

[37] Jankowski, R. (2005). Non-linear viscoelastic modelling of earthquake-induced structural pounding. *Earthquake engineering & structural dynamics*, **34**, 595–611. 92, 94

[38] Jankowski, R., Wilde, K. & Fujino, Y. (1998). Pounding of superstructure segments in isolated elevated bridge during earthquakes. *Earthquake Engineering & Structural Dynamics*, **27**, 487–502. 92

[39] Jankowski, R., Wilde, K. & Fujino, Y. (2000). Reduction of pounding effects in elevated bridges during earthquakes. *Earthquake Engineering & Structural Dynamics*, **29**, 195–212. 155

[40] Kasai, K., Jagiasi, A. & Jeng, V. (1996). Inelastic vibration phase theory for seismic pounding mitigation. *Journal of Structural Engineering*, **122**, 1136–1146. 155

[41] Kawashima, K. & Shoji, G. (2000). Effect of restrainers to mitigate pounding between adjacent decks subjected to a strong ground motion. **1435**. 155

[42] Kelly, J. (1991). Base isolation: origins and development. *News–Earthquake Engineering Research Center*, **12**, 1–3. 138

[43] Kelly, J. (1999). The role of damping in seismic isolation. *Earthquake engineering & structural dynamics*, **28**, 3–20. 138

[44] Kirkayak, L. (2009). *Numerical and Experimental Analysis of Container Stack Dynamics*. Ph.D. thesis, The University of Tokyo, Graduate School of Frontier Sciences. 6, 9, 25, 117

[45] Kirkayak, L., Suzuki, K., Sueoka, H., Aguiar, V.S., Masabayashi, K. & Ando, H. (2009). Dynamic simulation of container lashing behavior. *Conference of the Japan Society of Naval Architects and Ocean Engineers–JASNAOE*. 25

[46] Lee, H. & Ko, D. (2007). Seismic response characteristics of high-rise RC wall buildings having different irregularities in lower stories. *Engineering Structures*, **29**, 3149–3167. 31

[47] Levinson, M. (2006). *The Box: How the shipping container made the world smaller and the world economy bigger*. Princeton University Press. 4, 5

[48] Li, C., Lam, S., Zhang, M. & Wong, Y. (2006). Shaking table test of a 1: 20 scale high-rise building with a transfer plate system. *Journal of Structural Engineering*, **132**, 1732. 31

[49] Liu, M. & Gorman, D. (1995). Formulation of Rayleigh damping and its extensions. *Computers & Structures*, **57**, 277–285. 83

[50] Lu, X., Fu, G., Shi, W. & Lu, W. (2007). Shake table model testing and its application. *The Structural Design of Tall and Special Buildings*, **17**, 181–201. 31

[51] Midorikawa, M., Azuhata, T., Ishihara, T. & Wada, A. (2006). Shaking table tests on seismic response of steel braced frames with column uplift. *Earthquake engineering & structural dynamics*, **35**, 1767–1785. 31

[52] Mohammad, D., Khan, N. & Ramamurti, V. (1995). On the role of Rayleigh damping. *Journal of Sound and Vibration*, **185**, 207–218. 84

[53] Murdoch, E. & Tozer, D. (2006). A master guide to container securing. *Lloyd's Register and The Standard*. 7, 20, 21, 22, 23, 24

[54] Murty, K., Liu, J., Wan, Y. & Linn, R. (2005). A decision support system for operations in a container terminal. *Decision Support Systems*, **39**, 309–332. 25

[55] Nader, M. (1996). Shaking table tests of rigid, semirigid, and flexible steel frames. *Journal of Structural Engineering*, **122**, 589. 31

[56] Oshiro, R. & Alves, M. (2007). Scaling of cylindrical shells under axial impact. *International Journal of Impact Engineering*, **34**, 89–103. 52

[57] Pace, D. (2004). Modeling and simulation verification and validation challenges. *Johns Hopkins APL Technical Digest*, **25**, 163–172. 29

[58] Podsada, J. (2010). Lost sea cargo: Beach bounty or junk? *National Geographic*. 12

[59] Prasad, S., Towhata, I., Chandradhara, G.P. & Nanjundaswamy, P. (2004). Shaking table tests in earthquake geotechnical engineering. *Current Science*, **27**, 1398–1404. 31

[60] Qian, Y., Swanson, S., Nuismer, R. & Bucinell, R. (1990). An experimental study of scaling rules for impact damage in fibre composites. *Journal of Composite Materials*, **24**, 559–570. 52

[61] Raheem, S. (2006). Seismic pounding between adjacent building structures. *Electronic Journal of Structural Engineering*, **6**, 66. 155

[62] Rayleigh, B. (1896). *The theory of sound*. Macmillan. 86

[63] Rezaeepazhand, J., Simitses, G. & Starnes, J. (1995). Use of scaled-down models for predicting vibration response of laminated plates. *Journal of Composite Structures*, **30**, 419–426. 52

[64] Rezaeephazhand, J., Simitses, G. & Starnes, J. (1996). Design of scale down models for predicting shell vibration response. *Journal of Sound and Vibration*, **2**, 301–311. 52, 54, 159

[65] Rowlett, R. (2005). How many? a dictionary of units and measurements. `http://www.unc.edu/~rowlett/units/`. 17

[66] Ruangrassamee, A. & Kawashima, K. (2003). Control of nonlinear bridge response with pounding effect by variable dampers. *Engineering Structures*, **25**, 593–606. 155

[67] Samali, B., Wu, Y. & Li, J. (2003). Shake table tests on a mass eccentric model with base isolation. *Earthquake Engineering & Structural Dynamics*, **32**, 1353–1372. 31

[68] Semblat, J. (1997). Rheological interpretation of Rayleigh damping. *Journal of Sound and Vibration*, **206**, 741–744. 83

[69] Shakya, K., Wijeyewickrema, A. & Ohmachi, T. (2008). Mid-column seismic pounding of reinforced concrete buildings in a row considering effects of soil. In *14th World Conference on Earthquake Engineering: Innovation Practice Safety. International Association for Earthquake Engineering, Beijing, China*. 94

[70] Sharma, I. (????). *Seismic Pounding Effects in Buildings*. Ph.D. thesis, Department of Civil Engineering National Institute of Technology, Rourkela. 155

[71] Simitses, G. & Rezaeepazhand, J. (1993). Structural similitude for laminated structures. *Journal of Composites Engineering*, **3**, 751–765. 52

[72] Singhatanadgid, P. & Songkhla, A.N. (2008). An experimental investigation into the use of scaling laws for predicting vibration responses of rectangular thin plates. *Journal of Sound and Vibration*, **311**, 314–327. 52

[73] Soedel, W. (1971). Similitude approximations for vibrating thin shells. *The Journal of the Acoustical Society of America*, **49**, 1535–1541. 52

[74] Soong, T., Spencer, B. *et al.* (2002). Supplemental energy dissipation: state-of-the-art and state-of-the-practice. *Engineering Structures*, **24**, 243–260. 138

[75] Stahlbock, R. & Voss, S. (2008). Operations research at container terminals: a literature update. *OR Spectrum*, **30**, 1–52. 25

[76] Sun, Q., Zhang, L., Zhou, J. & Shi, Q. (2003). Experimental study of the semi-active control of building structures using the shaking table. *Earthquake engineering & structural dynamics*, **32**, 2353–2376. 31

[77] Suzuki, K., Kirkayak, L., Sueoka, H., Futaoka, Y., Masabayashi, K. & Ando, H. (2009). Model test of container lashing dynamic behavior. *Conference of the Japan Society of Naval Architects and Ocean Engineers–JASNAOE*. 25

[78] Taleb-Ibrahimi, M., De Castilho, B. & Daganzo, C. (1993). Storage space vs handling work in container terminals. *Transportation Research Part B: Methodological*, **27**, 13–32. 25

[79] Torkamani, S., Navazi, H., Jafari, A. & Bagheri, M. (2009). Structural similitude in free vibration of orthogonally stiffened cylindrical shells. *Thin-Walled Structures*, **47**, 1316–1330. 52

[80] Turpin, E. & MacEwen, W. (1965). *Merchant Marine officer's handbook*. Cornell Maritime Press. 17

[81] Ungbhakorn, V. & Singhatanadgid, P. (2003). Similitude and physical modeling for buckling and vibration of symmetric cross-ply laminated circular cylindrical shells. *Journal of Composite Materials*, **37**, 1697–1712. 52

[82] Ungbhakorn, V. & Singhatanadgid, P. (2003). Similitude invariants and scaling laws for buckling experiments on anti-symmetrically laminated plates subjected to biaxial loading. *Composite Structures*, **59**, 455–465. 52

[83] Valles, R. & Reinhorn, A. (1997). Evaluation, prevention and mitigation of pounding effects in building structures. *Technical Report NCEER*. 92

[84] van Teijlingen, E., Rennie, A., Hundley, V. & Graham, W. (2001). The importance of conducting and reporting pilot studies: the example of the Scottish Births Survey. *Journal of Advanced Nursing*, **34**, 289–295. 97

[85] Vassalos, D. (1999). Physical modelling and similitude of marine structures. *Ocean Engineering*, **26**, 111–123. 29, 49, 51, 52, 54

[86] Villaverde, R. & Mosqueda, G. (1999). Aseismic roof isolation system: analytic and shake table studies. *Earthquake Engineering & Structural Dynamics*, **28**, 217–234. 31

[87] Vis, I. & De Koster, R. (2003). Transshipment of containers at a container terminal: An overview. *European Journal of Operational Research*, **147**, 1–16. 25

[88] Weisstein, E.W. (2010). "root-mean-square."from mathworld–a wolfram web resource. http://mathworld.wolfram.com/Root-Mean-Square.html. 39

[89] Winter, D. (2009). *Biomechanics and motor control of human movement*. John Wiley & sons. 43, 45

[90] Wu, J.J. (2003). The complete-similitude scale models for predicting the vibration characteristics of the elastically restrained flat plates subjected to dynamic loads. *Journal of Sound and Vibration*, **268**, 1041–1053. 52

[91] Wu, J.J. (2005). Dynamic analysis of a rectangular plate under a moving line load using scale beams and scaling laws. *Computers and Structures*, **83**, 1646–1658. 52

[92] Wu, J.J. (2006). Prediction of the dynamic characteristics of an elastically supported full-size flat plate from those of its complete-similitude scale model. *Journal of Computers and Structures*, **84**, 102–114. 52

[93] Wu, J.J. (2007). Prediction of lateral vibration characteristics of a full-size rotor-bearing system by using those of its scale models. *Finite Elements in Analysis and Design*, **43**, 803–816. 52

[94] Wu, J.J., Cartmell, M. & Whittaker, A. (2002). Prediction of the vibration characteristics of a full-size structure from those of a scale model. *Computers and Structures*, **80**, 1461–1472. 52

[95] Wu, Y. & Samali, B. (2002). Shake table testing of a base isolated model. *Engineering Structures*, **24**, 1203–1215. 31

[96] ZHOU, Y., LU, X., LU, W. & HE, Z. (2009). Shake table testing of a multi-tower connected hybrid structure. *Earthquake Engineering and Engineering Vibration*, **8**, 47–59. 31

[97] ZHU, P., ABE, M. & FUJINO, Y. (2002). Modelling three-dimensional non-linear seismic performance of elevated bridges with emphasis on pounding of girders. *Earthquake Engineering & Structural Dynamics*, **31**, 1891–1913. xvii, 93, 94